

A review on hygrothermal white-box models of building envelopes in China

Tingting Zhang^{a,b,*}, Hartwig M. Künzel^b, Daniel Zirkelbach^b, Mingfang Tang^a, Kehua Li^c, Tobias Schöner^b, Jing Ren^a

^a School of Architecture and Urban Planning, Chongqing University, 400044 Chongqing, China

^b Department of Hygrothermics, Fraunhofer Institute for Building Physics, 83626 Holzkirchen, Germany

^c Midea Building Technology, Midea Group, 528311 Foshan, China

ARTICLE INFO

Keywords:

Moisture control
Durability
Hygrothermal white-box model
Hygrothermal reference year
Occupants' behavior

ABSTRACT

Moisture damage plays a key role for the durability of buildings and for the health and comfort of occupants. Various numerical models were proposed for engineers and architects to evaluate the hygrothermal condition before constructing in China. Although the physical discipline is universal, the complexity and variety of climates and building components make the moisture-related problems as well as the development and application of hygrothermal models distinctive in China. This paper is a comprehensive survey of the state-of-the-art in China to promote future advancement and academic communication between China and abroad. It investigated hygrothermal white-box models in China including modeling and input parameters. The paper presents that the assumptions of available models limit the application of hygrothermal white-box models in some situations. It also shows that there is a shortage of suitable indoor and outdoor climate databases. To sum up, the following items are necessary to establish hygrothermal simulation in building practice: models working with separate driving potentials for liquid and vapour transport; hygrothermal reference years as outdoor climate data; indoor climate data, either measured occupants' behavior or derived from building operation setpoints influenced by outdoor climate.

1. Introduction

1.1. Moisture-related problems in China

In China, the outdoor climate in different regions covers a large spectrum because of the huge territory. The complexity and variety of occupants' activities may also make the indoor hygrothermal environment unique [1] which means it differs from conditions recorded in Europe and North America. Modern constructions under Chinese standards of five climatic zones [2–5] and heritage constructions composed of traditional materials [6] are faced with largely unknown outdoor and indoor climatic loads [7,8].

Walls of traditional buildings are normally single-layer structures composed of clay, wood or brick, etc. and there was no insulation and HVAC system in the past. Since there is no distinct temperature and moisture gradient between outdoor and indoor climate, moisture damage detected on heritage buildings is caused by wind-driven rain (WDR) penetration or high relative humidity (RH) exposure [10,11].

Owing to HVAC operation and installation of insulation materials

[12–14], modern buildings are facing further moisture-related problems. In the north of China, interstitial condensation in building envelopes is likely to appear when heating systems work in wintertime. The impact of WDR or condensation water, which cannot dry out fast enough, may lead to freeze–thaw damage under fluctuating heat and moisture loads [15]. In the south of China, it is possible to observe surface condensation on floors when the floor temperature is lower than the dew-point temperature of the ambient air, e.g. cement-based ground floor of residential buildings in the countryside in Chongqing [16]. Mould growth had also been observed in Shanghai due to high air humidity [17].

In addition, except for buildings in mild zone without HVAC system and insulation material [2–5], the indoor temperature and humidity in other zones are often lower than the outdoor conditions, since the cooling system works in summertime. This poses a high risk on the colder side of building envelopes [18], especially when they are exposed to WDR and solar radiation. Interstitial condensation may occur on colder surfaces due to the so-called vapour drive effect [19].

All of these moisture-related problems change the thermal performance of building envelopes, which can influence HVAC performance

* Corresponding author at: School of Architecture and Urban Planning, Chongqing University, 400044 Chongqing, China.

E-mail address: 20201501014@cqu.edu.cn (T. Zhang).

Nomenclature	
j_m	moisture flux density (kg/m ²)
j_v	vapour diffusion flux density (kg/m ²)
j_l	liquid water flux density (kg/m ²)
j_e	moisture flow density on the exterior surface (kg/m ²)
j_a	air flux (kg/m ²)
P_v	partial pressure of water vapor (Pa)
P_{sat}	saturation vapor pressure (Pa)
P_a	total air pressure (Pa)
$P_{e,a}$	vapour pressure of outdoor air (Pa)
$P_{e,sur}$	vapour pressure on the exterior surface (Pa)
s	capillary pressure (Pa)
R	gas constant (J/kg K)
T	temperature (K)
$T_{e,a}$	temperature of outdoor air (K)
$T_{e,sur}$	temperature on the exterior surface (K)
T_{wdr}	temperature of wind-driven rain (K)
T_{sur}	temperature of the exterior surface (K)
T_0	absolute minimum temperature of mould growth (K)
T_n	temperature of the nth datum higher than critical condition (K)
r	capillary radius (r)
w	moisture content (kg/m ³)
X	humidity ratio (kg/kg)
q	total heat flux density (W/m ²)
q_e	heat flux density on the exterior surface (W/m ²)
$q_{e,rad}$	heat flux density due to solar radiation (W/m ²)
q_{cr}	correction rate (-)
q'	heat flux density without moisture load (W/m ²)
h_v	latent heat of evaporation (J/kg)
c	total specific heat of capacity (J/kg K)
c_l	specific heat capacity of liquid water (J/kg K)
c_v	specific heat capacity of vapour pressure (J/kg K)
H_v	enthalpy of vapour pressure (J/kg)
H_l	enthalpy of liquid water (J/kg)
w_v	vapour content (kg/m ³)
V	volume (m ³)
t	time (s)
Q_{tran}	heat flow due to solar radiation and the heat fluxes due to convection and transfer within the building envelopes (W)
Q_{pro}	heat production from occupants and equipment (W)
Q_{vent}	heat fluxes due to ventilation (W)
Q_{flow}	heat fluxes due to air flow in multi-zone (W)
Q_{HVAC}	heat fluxes due to operation of HVAC (W)
v_i	absolute humidity ratio of the interior air (kg/m ³)
W_{tran}	moisture fluxes due to exchange and transfer with building envelopes (kg/h)
W_{pro}	moisture production from occupants and equipment (kg/h)
W_{vent}	moisture fluxes due to ventilation (kg/h)
W_{flow}	moisture fluxes due to air flow among zones (kg/h)
W_{HVAC}	moisture fluxes due to operation of HVAC (kg/h)
R_{wdr}	wind-driven rain load (kg/m ² s)
R_{runoff}	runoff rain load (kg/m ² s)
S_{RH80}	index of mould growth risk (-)
RH_0	relative humidity of the nth datum higher than 80 % (-)
RH_n	absolute minimum relative humidity of mould growth (-)
n	number of data (-)
Greeks	
δ_v	water vapor permeability (kg/m s pa)
δ_l	liquid water permeability (kg/m s pa)
δ_x	equivalent total moisture diffusion coefficient at X axis (kg/m s pa)
δ_y	equivalent total moisture diffusion coefficient at Y axis (kg/m s pa)
δ_a	vapour permeability of air (kg/m s pa)
ϕ	relative humidity (-)
ρ	total density (kg/m ³)
ρ_l	density of liquid water (kg/m ³)
σ	surface tension of water (N/m)
θ	contact angle (°)
ε	porosity of building material (-)
λ	thermal conductivity (W/m K)
μ	vapor diffusion resistance factor (-)
ξ_c	specific moisture content (kg/m ³)
ε	thermogradient coefficient (kg/m ³ K)
η	ratio of vapor diffusion coefficient to coefficient of total moisture diffusion (-)
γ	heat of absorption or desorption (kJ/kg)
α_c	convective coefficient (W/m ² K)
β_e	mass exchange coefficient on the exterior surface (m/s)
$\alpha_{e,rad}$	absorptivity of solar radiation (-)
Abbreviations	
RH	relative humidity (-)
WDR	wind-driven rain (-)
CNKI	China National Knowledge Infrastructure (-)
CQVIP	China Science and Technology Journal Database (-)
TMY	Typical Meteorological Year (-)
1D	One-dimensional (-)
2D	Two-dimensional (-)
3D	Three-dimensional (-)
CFD	computational fluid dynamics (-)

due to the change in heat loss and gain. Also the indoor climate might not meet the comfort and health requirement by following the standard operation mode of HVAC system [20].

1.2. State of the art in China

These typical phenomena in China are not yet sufficiently represented in international and universal tools such as WUFI Pro developed in Germany [21]. Chinese scholars make a contribution to developing new hygrothermal white-box models, which are characteristic for China. Although the physical process is the similar, e.g. heat and moisture transfer models are based on Fourier's law, Darcy's law and Fick's law, the difference of assumption and simplification in hygrothermal models

makes models match different application cases better. For instance, models considering hysteresis were proposed for bio-based materials, which can be applied to evaluate heritage timber buildings [22–24]. In the north of China, models with ice formation are needed and considered by Kong et al. [15]. It is meaningful that Chinese scholars proposed hygrothermal models targeting on specific Chinese climate and components with traditional materials.

However, to decrease orders of coupled heat and moisture equations, Chen et al. assumed the vapour conductivity and equivalent thermal conductivity to be constants to transform the equations into linear partial differential equations with one order [25]. The simplification of this method ignores the moisture effects on thermal resistance and the analysis of smart vapour retarders that change their vapour permeability

according to ambient RH conditions, so the application for a large range of RH is limited.

Therefore, there are pros and cons for Chinese models compared with tools or models abroad. The analysis concerning the accuracy of models based on different assumptions and application situations of different constructions in China is necessary.

China National Knowledge Infrastructure (CNKI) [26], Wanfang [27] and China Science and Technology Journal Database (CQVIP) [28] collect publications partially written in Chinese dealing with the topic of hygrothermal white-box models developed by Chinese researchers. Overseas researchers cannot access these publication databases. Relevant papers in Chinese journals [25,29–33], handbooks [34], textbooks [35–37] and standards [2–5,38,39] are mostly in Chinese. It is challenging to spread these research achievements to other countries.

1.3. Classification of modeling system

There are three types of modeling systems including white-box, grey-box and black-box system theories. White-box means all parameters, the connections of parameters, and even the physical processes are transparent and clear. Grey-box means parameters, connections of parameters and the physical processes are only partially known or derived from empirical studies. Those have been applied for some earlier research. Black-box means nothing or very little is known about the theory and assumptions of the underlying method. Scholars rely on the input and output to analyze the discipline of the whole analysis system [41]. Most analyses are based on a white-box system theory, so this paper mainly focuses on discussing white-box system.

1.4. Objectives

This paper is a systematic survey of current Chinese research results of hygrothermal models, which guides users to select suitable models for different simulation purposes and makes potential perspectives clear. It also provides possibilities for scholars abroad to get to know the development of hygrothermal white-box models in China.

2. Methodology

After classifying, analyzing and concluding, we have a framework to show our research methodology of this paper, shown in Fig. 1. It is organized into four phases.

Phase one: Overview of moisture loads in China because of modeling consideration depending on different complexity.

Phase two: Summary of modeling in China and comparison with published and established models in other countries.

Phase three: Analysis of input parameters and comparison with corresponding measurement methodology in standards from other countries.

Phase four: Investigation of model application in China and suggestion of improvements and model selection for relevant cases.

3. Moisture loads in China

Outdoor and indoor moisture loads are key moisture sources. The exterior moisture load mainly including moist air and WDR is determined by meteorological parameters, which are mainly influenced by

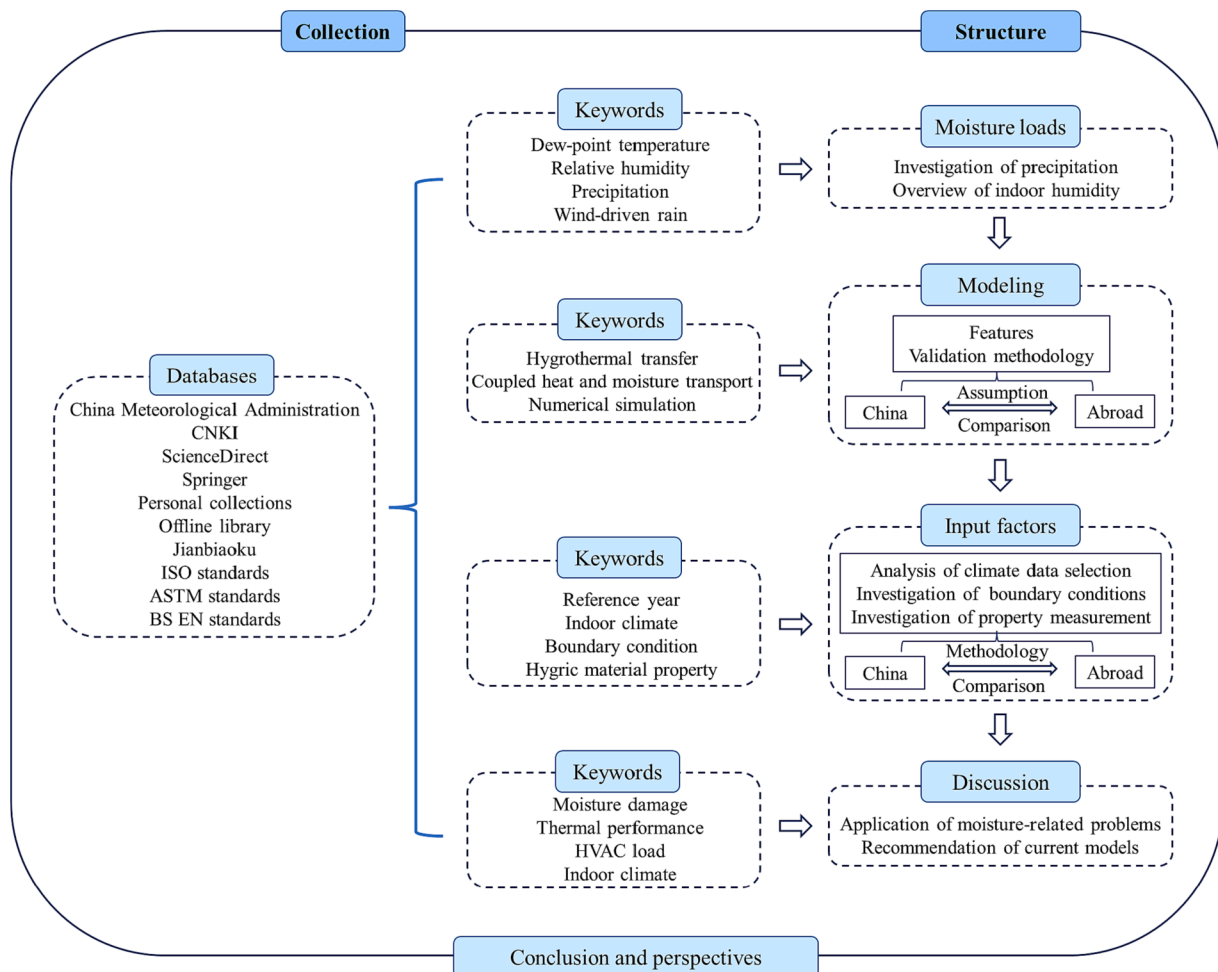


Fig. 1. Framework of the review including databases in China and abroad, the searched keywords in different chapters.

altitude, latitude, proximity to the ocean, topography, etc.. The interior moisture load mainly focusing on moist air is a function of outdoor environment, building envelope performance, indoor hygrothermal loads and HVAC system, with the last two being strongly influenced by occupants' behavior. Due to the difference of tradition and culture (e.g. cooking), the habit to open windows, use humidification or dehumidification equipment, HVAC system, etc. strongly varies from country to country. Therefore, outdoor and indoor loads are different to North America and Europe or even other countries in Asia.

China is located in the east of Asia with the Pacific Ocean in the east and the Himalaya in the west. The survey from China Meteorological Administration shows that the annual precipitation in the south is more than 900 mm. In the north of China, the annual precipitation is less than 600 mm such as Heilongjiang [42], which is lower than Vancouver in Canada around 1000 mm with similar latitude [43]. Based on the mean values of outdoor temperature in coldest and hottest months, GB 50176 classifies China into five climatic zones: severe cold zone, cold zone, hot summer and cold winter zone, hot summer and warm winter zone, mild zone [39]. The annual precipitation in different climatic zones is shown in Fig. 2. There are high WDR exposure risks for buildings in the southeast of China based on surveys [44], shown in Fig. 3.

The long-term observation of interior moisture loads is rare in China. Based on the four-day observation in 9 cities, the cumulative frequency of indoor RH in residential buildings varies from city to city [45]. Cities in the south such as Shanghai, Changsha and Chongqing face high indoor humidity conditions as shown in Figs. 4 and 5. In summer, the indoor RH in Shanghai is mainly between 60 % and 80 %, which is higher than Kyushu mainly between 40 % and 60 % with similar latitude in Japan [46].

4. Hygrothermal white-box models in China

4.1. General features

4.1.1. Modeling establishment

The heat and moisture transfer process are complex. To simplify hygrothermal models, typical assumptions are listed below:

- (1) Building materials are homogeneous.
- (2) Moisture properties of building materials are only related to ambient humidity.
- (3) The hysteresis effect on the sorption isotherm is neglected.

(4) The effect of gravity in the envelope and convection in building material pores are not considered.

(5) Water vapour is assumed as ideal gas.

(6) Thermodiffusion by temperature gradient is negligible.

(7) Density and specific heat capacity of dry building materials are constants.

Based on those assumptions, models normally contain mass and energy conservation equations, with storage term being on the left and transport terms on the right sides of the differential equations. Heat transport in heat balance equation follows Fourier's law. Moisture transport in moisture balance equation contains liquid transport and vapour diffusion. The former follows Darcy's law or similar approaches and the latter follows Fick's law, shown in Fig. 6.

4.1.2. Validation methodologies

Since the research of three-dimensional models are rare, the modeling and validation are mainly one and two-dimensional models. There are two methods: the first one is comparison with suitable and well-documented experiments. The second one is comparison with benchmarks. Temperature, RH and moisture content are generally compared. The agreement is evaluated by statistical criteria.

A common experimental protocol is to expose a sample component to one or two fluctuating climate conditions, shown in Fig. 7. The climate data on one or two sides of sample components are boundary conditions for calculation of models.

Unfortunately, there is no published benchmark to validate new hygrothermal white-box models in China, so EN 15026 [47], HAMSTAD [48] and literature [49,50] including material properties and various components, such as single-layer and multi-layer structure, are referred to by Chinese scholars [51–53]. The first two provide calculation results from European organizations. The last one is based on measurement from overseas authors. All benchmarks are for one-dimensional models.

Statistical indexes, such as root mean square error and coefficient of determination, shows the discrepancy between benchmarks or the experiment and calculative results, which reflects the reliability of models [54]. Low root mean square error and high coefficient of determination means models are sufficiently accurate. There is no definition of thresholds to show the range of agreement such as excellent level to low level.

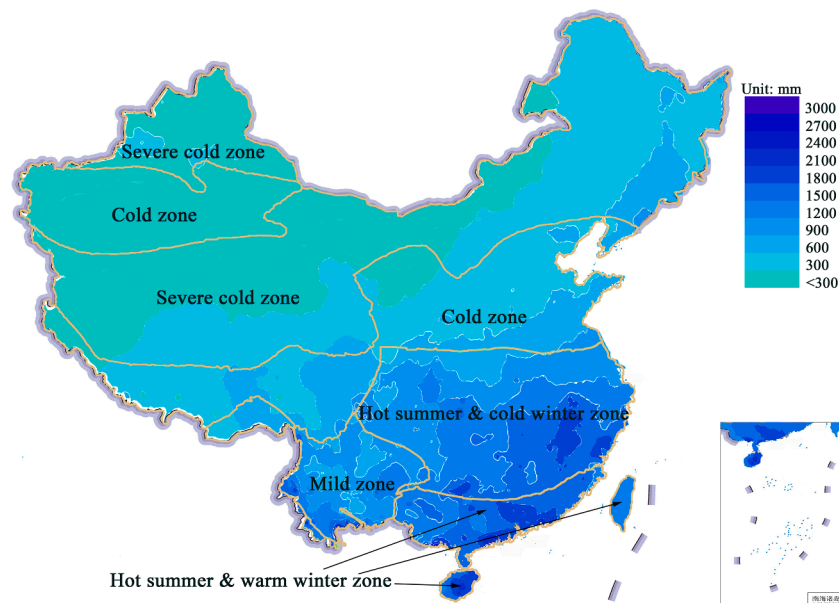


Fig. 2. Annual precipitation in different climatic zones in China, the southeast is more than 900 mm, while the northwest is less than 300 mm [39].

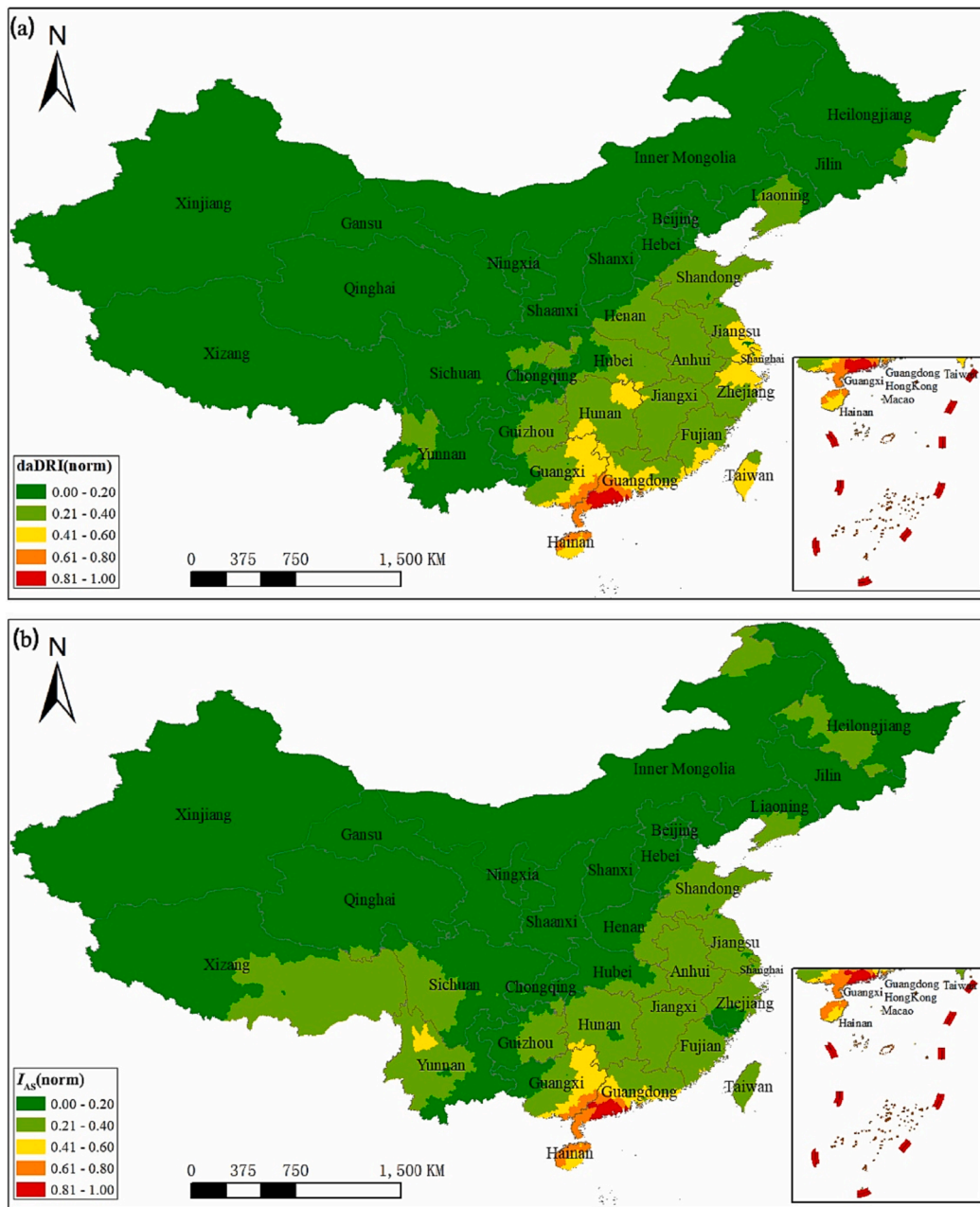


Fig. 3. Standardized WDR exposure map, the overall results show agreement with the distribution of annual precipitation: (a). long-term exposure; (b). extreme exposure [44].

4.2. Investigation of modeling assumptions

Buildings are required to be airtight to theoretically avoid heat loss and the heat, air and moisture flow on exterior and interior surfaces is separately dealt with outdoor and indoor boundary conditions, respectively. The component is simplified without cavity and boundary or to be perfectly sealed, so airflow such as exfiltration, infiltration, cavity ventilation, wind washing, indoor air washing and air looping in buildings is ignored. Therefore, we focus on analyzing the heat, air and moisture flow through open pore materials.

4.2.1. Moisture transport

Moisture flow includes vapour water flow by diffusion and liquid water flow by capillary suction. The moisture convection through materials is weak, so the moisture convection is assumed together with moisture source in some cases.

Transport mechanisms including air pressure and gravity are negligible, so driving potentials of moisture transport, relevant to calculations in building physics, are differences in vapour pressure and in capillary pressure or suction pressure for vapour diffusion and liquid transport, respectively.

Therefore, the moisture transport process based on mass conservation can be described as:

$$j_m = j_v + j_l \quad (1)$$

where j_m is the moisture flux density; j_v the vapour diffusion flux density; j_l the liquid water flux density. Dong et al. supposed that thermodiffusion (moisture transport under temperature gradient) existed [9]. However, research based on experimental data collected by Belgium scholar, Hans Janssen, shows only a very limited relevance of this effect under the conditions acting on buildings in practice [55]. Therefore, it

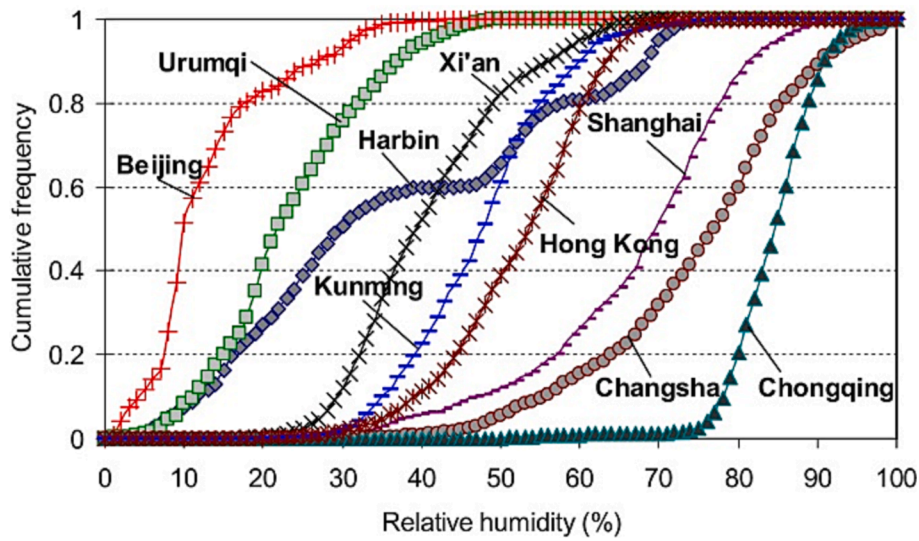


Fig. 4. Indoor RH in 9 cities in China in winter [45].

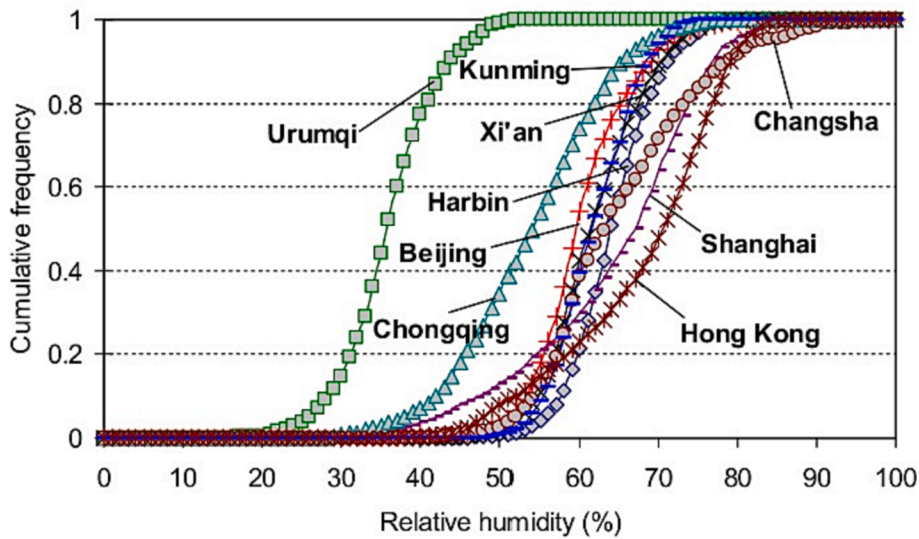


Fig. 5. Indoor RH in 9 cities in China in summer [45].

can be assumed that thermodiffusion is negligible in the scope of building science. Then the vapour diffusion flux density can be described via Eq. (2) based on Fick's law:

$$j_v = -\delta_v \nabla P_v \quad (2)$$

where δ_v is the water vapour permeability; P_v the partial pressure of water vapour. Chen et al. supposed that vapour permeability was constant and temperature-independent [29], which is not beneficial to guide the installation of vapour retarder introduced in ASHRAE handbook [56] and the application of smart vapour retarder. By referring to Darcy's law, the liquid water flux density can be given as:

$$j_l = -\delta_l \nabla s \quad (3)$$

where δ_l is the liquid water permeability; s the capillary pressure. The total moisture transport, which the vapour diffusion with driving potential is difference of vapour pressure and liquid transport with driving potential is difference of capillary pressure, can be described as:

$$j_m = -(\delta_v \nabla P_v + \delta_l \nabla s) \quad (4)$$

When the difference of vapour pressure is assumed as constant and

liquid transport is disregarded, Eq. (4) can describe Glaser's method that Chinese standard GB 50176 recommends [39], which is far from the real condition.

There are various models in China, we organize different types of models from the relation of different driving potentials in this paper. Since the water vapour is ideal gas based on the assumption, RH can be described as:

$$\phi = \frac{P_v}{P_{sat}} \quad (5)$$

where ϕ is the RH; P_{sat} the saturation vapour pressure. According to Kelvin's equation:

$$s = \rho_l RT \ln(\phi) \quad (6)$$

where ρ_l is the density of liquid water; R the gas constant; T the temperature. If building materials are homogeneous, the function of capillary by radii can be theoretically used in Eq. (7).

$$s = 2\sigma \cos \frac{\theta}{r} \quad (7)$$

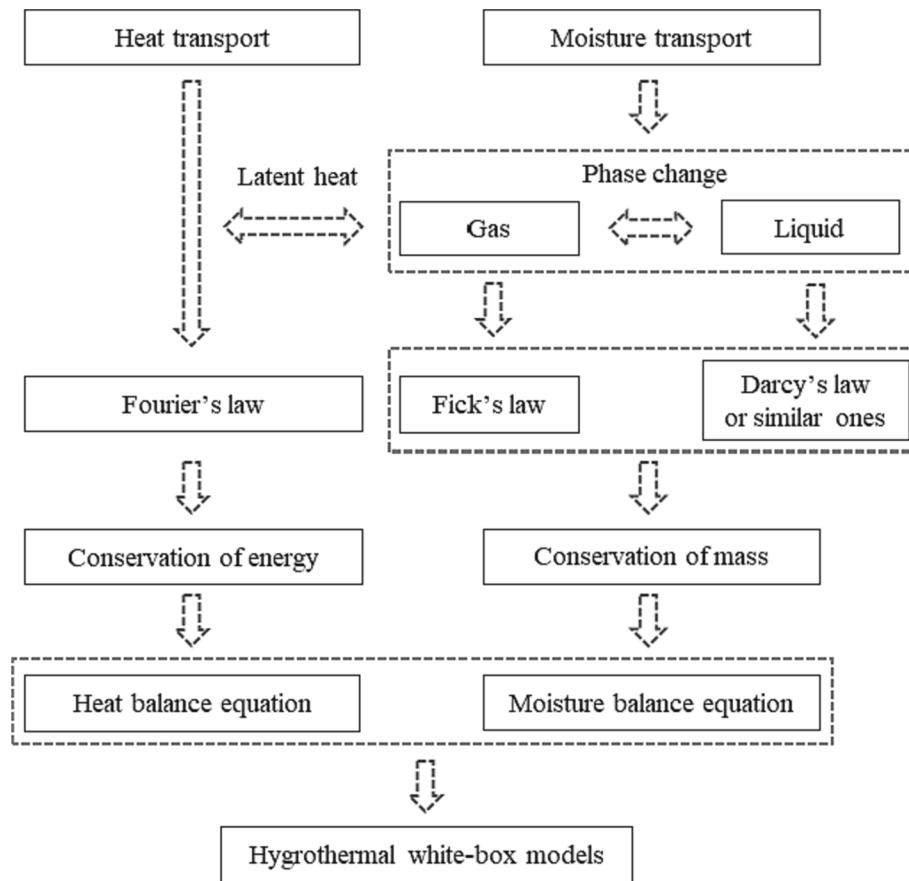


Fig. 6. The general features of hygrothermal white-box models including heat transport and moisture transport which are mutually coupled by latent heat.

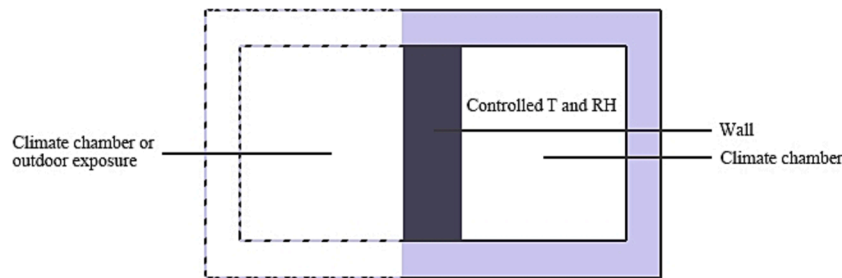


Fig. 7. Measurement protocol of validation for white-box hygrothermal models.

where σ is the surface tension of water; θ the contact angle; r the capillary radius. However, as the pores in building materials are not evenly [57], this would lead to coarse evaluation. It is better to test capillary pressure directly. Therefore, Eq. (7) that the capillary pressure relying on pore radii is not suggested. Eq. (4) can be transformed as:

$$j_m = -(\delta_v \nabla P_v + \delta_l \nabla(\rho_l RT \ln(\frac{P_v}{P_{sat}}))) \quad (8)$$

where the driving potential is only the difference of vapour pressure to simplify the calculation. At the same time, Eq. (4) can also be transformed as:

$$j_m = -(\delta_v \nabla(\phi P_{sat}) + \delta_l \nabla(\rho_l RT \ln(\phi))) \quad (9)$$

where the potential is only the difference of RH. Zhang et al. [22–24], Liu et al. [58], Kong et al. [15] and Wang et al. [40] applied this method similar to Hartwig M. Künzels model which is the basis of the software of WUFI family in Germany [21]. If Eq. (9) is solved, ϕ , P_{sat} and T are

variables, it is given as:

$$j_m = -\left(\delta_v(\phi \nabla P_{sat} + P_{sat} \nabla \phi) + \delta_l\left(\rho_l RT \ln(\phi) \nabla T + \frac{\rho_l RT}{\phi} \nabla \phi\right)\right) \quad (10)$$

By referring to the method in literature [59], although the definition of ∂T and ∇T are different, they are the same based on the calculation law. Eq. (10) is equal to Eq. (11),

$$j_m = -(\delta_v(\phi \frac{\partial P_{sat}}{\partial T} \nabla T + P_{sat} \nabla \phi) + \delta_l(\rho_l RT \ln(\phi) \nabla T + \frac{\rho_l RT}{\phi} \nabla \phi)) \quad (11)$$

According to Eq. (2) and (5),

$$\begin{aligned} j_v &= -\delta_v(\phi \nabla P_{sat} + P_{sat} \nabla \phi) \\ &= -\delta_v(\phi \frac{\nabla P_{sat}}{\nabla T} \nabla T + P_{sat} \nabla \phi) \end{aligned}$$

$$= -\delta_v(\phi) \frac{\nabla P_{sat}}{\nabla T} \nabla T + P_{sat} \frac{\nabla \phi}{\nabla w} \nabla w \quad (12)$$

where w is the moisture content. Specific heat capacity illustrates the heat storage capability of a material. Similarly, moisture capacity reflects the moisture storage capability of porous materials. It illustrates the change in material moisture content by changes in environmental moisture. When relative humidity represents environmental moisture, the moisture capacity is usually characterized by the equilibrium moisture sorption curve. When capillary pressure represents environmental moisture, the moisture capacity may be characterized by a moisture storage function over capillary pressure or pore size. The general term for both representations is moisture retention curve. It spans the moisture content between 0 % and 100 % RH, respectively between infinite and zero capillary pressure. The moisture capacity is usually not constant but a function of RH determined from the slopes of equilibrium moisture sorption curve and moisture retention curve, which can be given by $\xi_\phi^w = \frac{dw}{d\phi}$ and $\xi_s^w = \frac{dw}{ds}$, Eq. (12) can be expressed as:

$$j_v = -\delta_v(\phi) \frac{\nabla P_{sat}}{\nabla T} \nabla T + \frac{P_{sat}}{\xi_\phi^w} \nabla w \quad (13)$$

The same method can be applied in Eq. (3) for liquid water transport,

$$j_l = -\delta_l \frac{ds}{dT} \nabla T \quad (14)$$

By referring to Kelvin's equation, $\frac{ds}{dT} = \rho_l R \ln(\phi)$ and according to the Eq. (4), (13) and (14), the moisture transport process based on mass conservation can be described via:

$$j_m = -\delta_v(\phi) \frac{\nabla P_{sat}}{\nabla T} \nabla T + \frac{\delta_l}{\delta_v} \rho_l R \ln(\phi) \nabla T + \frac{P_{sat}}{\xi_\phi^w} \nabla w \quad (15)$$

$\frac{\nabla P_{sat}}{\nabla T}$ can refer to empirical formula, such as Dillley's equation [60], then the driving potential is temperature and moisture content or volumetric moisture ratio in Eq. (15).

Authors also find an interesting application of humidity ratio being driving potential in the publication from Zhang et al. [61]. However, if the density of vapour is assumed as constant and liquid transport is negligible. Since the porosity is fixed, the volumetric moisture ratio, being the driving potential of vapour transfer, can be transformed into the humidity ratio by Eq. (16).

$$\begin{aligned} \nabla w &= \nabla(\varepsilon \rho_v X) \\ &= \varepsilon \rho_v \nabla X \end{aligned} \quad (16)$$

where ε is the porosity of building material; ρ_v the density of vapour; X the humidity ratio.

4.2.2. Heat transport

Heat transport includes the heat flux due to temperature difference which follows Fourier's law, and the latent heat due to phase change when evaporation and condensation occur. Compared with conduction and phase change, convection, radiation and internal energy of vapour are weak and negligible in airtight buildings. The latent heat is modeled as heat source or sink. Eq. (17) is usually used to describe the heat transport:

$$q = -(\lambda \nabla T + h_v \delta_v \nabla P_v) \quad (17)$$

where q is the heat flux density; λ the thermal conductivity.

Thermal conductivity shows a linear rise with temperature, the impact of moisture can also be approximated by a linear function given in [62] in the lower moisture range. The heat of evaporation h_v is temperature-dependent and pressure-dependent. It can be assumed as functions of temperature under normal air pressure, which Kong et al. [15], Liu et al. [58], Zhang et al. [61], Wang et al. [63] referred to. Qin

et al. [64], Zhang et al. [22], Wang et al. [40] assumed it as constants.

4.2.3. Airflow

The driving potential of airflow through open porous material is air pressure difference. It is normally given by air permeability and gradient in total air pressure [56], described by Eq. (18). Liu assumed that the velocity of airflow from one side to another side through open pores of materials is constant, which means $\nabla(\delta_a \nabla P_a)$ is equal to zero [65].

$$j_a = -\delta_a \nabla P_a \quad (18)$$

where j_a is the air flux density; δ_a the air permeability; P_a the partial pressure of air.

4.3. Representative models

Hygrothermal white-box models can be extended to one, two, three-dimensional according to the direction of gradient. One-dimensional (1D) models are used to describe the transfer direction perpendicular to the building envelope, so the gradient is assumed on X axis. Two-dimensional (2D) models are used to describe the transfer direction perpendicular and parallel to the building envelope, so the gradient is assumed on X axis and Y axis. Three-dimensional (3D) models are used to describe transfer direction occurring in corners such as thermal bridge. Available models are shown in Table 1. In Chapter 4.2.1, the relation among different moisture driving potentials is analyzed and related to models in Europe and the North America. Below are some representative models to show different moisture driving potential assumptions, consideration, validation and limitations in China:

(1) Relative humidity

Zhang et al. used relative humidity as single driving potential to propose models with temperature-dependent hysteresis-effect [22–24]. Models are presented as:

$$\frac{\partial w}{\partial \phi} \frac{\partial \phi}{\partial t} + \frac{\partial w}{\partial T} \frac{\partial T}{\partial t} = \frac{\partial}{\partial x} \left[\frac{\delta_a}{\mu} \frac{\partial(\phi P_s)}{\partial x} \right] \quad (19)$$

$$\rho_d c_d \frac{\partial T}{\partial t} + w c_l \frac{\partial T}{\partial t} = \frac{\partial}{\partial x} \left(\lambda \frac{\partial T}{\partial x} \right) + [\Delta h_v + (c_v - c_l)(T - 273.15)] \frac{\partial}{\partial x} \left(\frac{\delta_a}{\mu} \frac{\partial(\phi P_s)}{\partial x} \right) \quad (20)$$

where δ_a is the vapour permeability of air; μ vapour diffusion resistance factor; c_l the specific heat capacity of liquid water; c_v the specific heat capacity of vapour. Models were compared with measurement. One side of a 258.47 mm (L) x 98.82 mm (W) x 10.03 mm (T) wood plank was exposed to ambient air and another was airtight. Zhang et al. supposed that their models could better show the decreased trend of moisture content [23], compared with other researcher's models (shown in Fig. 8 (a), (b), (c)), when preset temperature decreased in the lab, shown in Fig. 8 (d).

(2) Capillary pressure

Fang et al. used capillary pressure as single driving potential for both vapour and liquid transport to predict WDR penetration [53]. Models are presented as:

$$\frac{\partial w}{\partial s} \frac{\partial s}{\partial t} = \nabla \left[\phi \frac{\partial P_{sat}}{\partial T} \nabla T + \left(-\delta_l - \delta_v P_{sat} \frac{\phi}{\rho_l RT} \right) \nabla s \right] \quad (21)$$

$$\begin{aligned} (\rho_d c_d + c_m w) \frac{\partial T}{\partial t} = \nabla \left[\left(\lambda + H_v \delta_v \phi \frac{\partial P_{sat}}{\partial T} \right) \nabla T + \left(-H_l \delta_l \right. \right. \\ \left. \left. - H_v \delta_v P_{sat} \frac{\phi}{\rho_l RT} \right) \nabla s \right] \end{aligned} \quad (22)$$

where H_v is the specific enthalpy of water vapour; H_l specific enthalpy of liquid water. These models were compared with benchmarks in HAM-STAD, shown in Fig. 9. Statistical index was not applied for these cases.

(3) Moisture content

Table 1
Information of hygrothermal white-box models in China.

Moisture driving potentials	Studies	Storage			Hysteresis	Transport			Envelope	Validation	Comments
		Vapour	Liquid water	Ice		Vapour permeability	Liquid permeability	Air movement			
RH	Zhang et al. [22–24]	✓	✓		✓	✓	✓	1D	Measurement		
	Liu et al. [58]	✓	✓			✓	✓	1D	Benchmark		
	Kong et al. [15]	✓	✓	✓		✓	✓	1D	Benchmark		
	Wang et al. [40]	✓	✓			✓	✓	1D	Benchmark		
RH and T	Chen et al. [9,52,66,67]	✓	✓			✓	✓	1D	Measurement		
RH, T and kinetic energy	Liu [65]	✓	✓			✓	✓	1D	Measurement		
Vapour pressure	Chen et al. [29]	✓				✓		1D		Limited application for a large range of RH	
Capillary pressure	Fang et al. [53]	✓	✓			✓	✓	1D	Benchmark		
Vapour content	Qin et al. [68]	✓				✓		2D	Measurement	Limited application for liquid water transfer	
	Zhang et al. [32]	✓				✓		1D	Measurement	Limited application for liquid water transfer	
Humidity ratio	Zhang et al. [61]	✓				✓		1D	Measurement	Limited application for liquid water transfer	

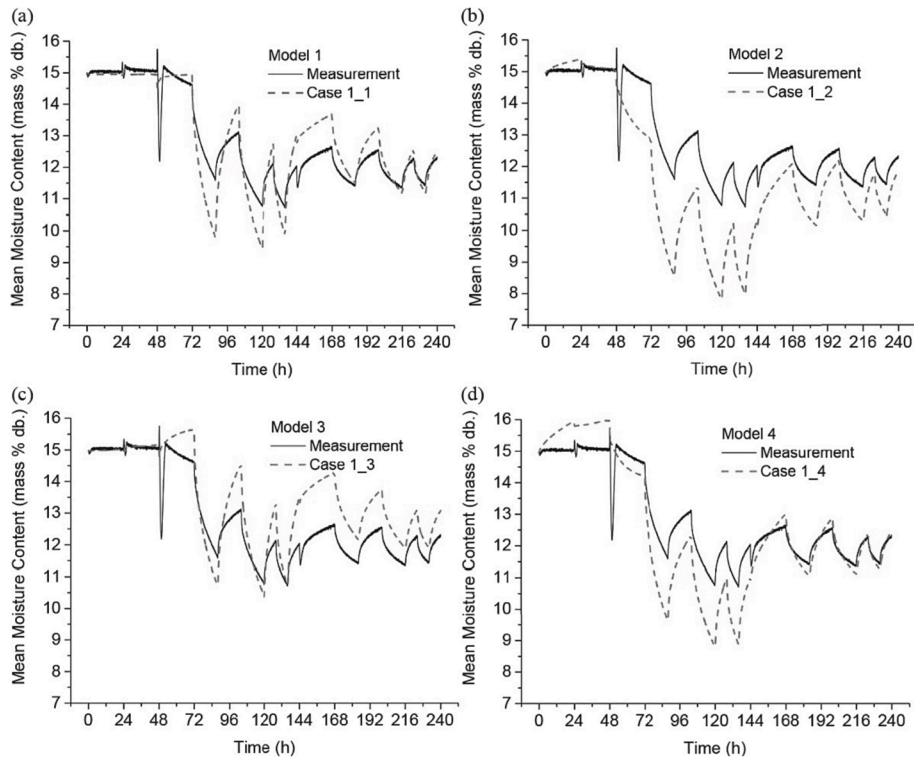


Fig. 8. Validation results for moisture content response of models with relative humidity being moisture driving potential proposed by Zhang et al., which models considered hysteresis and temperature-dependency [23].

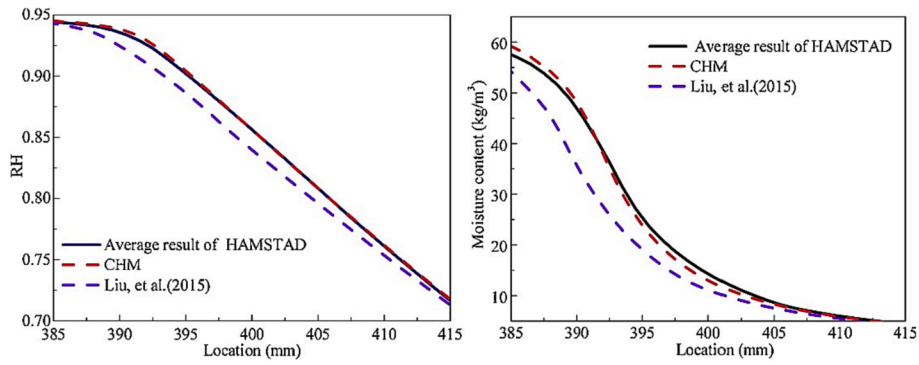


Fig. 9. The comparison results from HAMSTAD, models proposed by Liu et al. [66] and models proposed by Fang et al. with capillary pressure being moisture driving potential at the 60th calculation day [53].

Qin et al. used partial vapour content as single driving potential to propose 2D models, which might be applied on thermal bridge [68]. Models are presented as:

$$\frac{\partial w_v}{\partial t} = \frac{\partial}{\partial x} \left(\frac{\delta_x}{\rho \xi_c} \frac{\partial w_v}{\partial x} \right) + \frac{\partial}{\partial y} \left(\frac{\delta_y}{\rho \xi_c} \frac{\partial w_v}{\partial y} \right) + \frac{\partial}{\partial x} \left(\frac{\epsilon \delta_x}{\rho \xi_c} \frac{\partial T}{\partial x} \right) + \frac{\partial}{\partial y} \left(\frac{\epsilon \delta_y}{\rho \xi_c} \frac{\partial T}{\partial y} \right) \quad (23)$$

$$\frac{\partial T}{\partial t} = \frac{\partial}{\partial x} \left(\frac{\lambda_x}{\rho c} \frac{\partial T}{\partial x} \right) + \frac{\partial}{\partial y} \left(\frac{\lambda_y}{\rho c} \frac{\partial T}{\partial y} \right) + \frac{\xi_c}{c} (\eta h_v + \gamma) \frac{\partial w_v}{\partial t} \quad (24)$$

where w_v is vapour content; δ_x and δ_y equivalent total moisture diffusion coefficient at X axis and Y axis; ξ_c the specific moisture content; c the specific heat of capacity; ϵ quotient between thermal diffusion coefficient due to the temperature gradient and equivalent total moisture diffusion coefficient; η the ratio of vapour diffusion coefficient to coefficient of total moisture diffusion; γ the heat of absorption or desorption.

There is no benchmark for two dimensional models, model of moisture balance is validated by measurement [68]. A sample wall with saturated water was put between two chambers where the temperature was maintained as 20°C and the RH was 65 % in one chamber and 90 % in another. The sample was sealed except for the top and the bottom to make sure the moisture transport was not on horizontal level which was 1D, shown in Fig. 10. This measurement monitored the 2D moisture transport since there was difference of RH between the two chambers, but the temperature distribution was difficult to monitor, so only the moisture conservation equation was validated, the result is shown in Fig. 11. The statistical index was not applied. Models were assumed to be reliable when the tendency of the two figures was the same.

(5) Humidity ratio

Zhang et al. used humidity ratio as driving potential to predict the moisture buffering effect of straw-based board in civil defense shelter [69], while this would lead to deviation out of sorption isotherm when the RH is higher than 95 % or walls are oriented to WDR. Models are presented as:

$$\epsilon \rho_v \frac{\partial X}{\partial t} = \frac{\partial}{\partial x} \left(\delta_v \frac{\partial X}{\partial x} \right) - \frac{\partial w(X, T)}{\partial t} \quad (25)$$

$$C_d \rho_d \frac{\partial T}{\partial t} = \frac{\partial}{\partial x} \left(\lambda \frac{\partial X}{\partial x} \right) + h_v \frac{\partial w(X, T)}{\partial t} \quad (26)$$

here, one side of the sample wall is exposed to ambient air and another is airtight. A similar protocol is also used to check the performance of interior insulation system [13] to avoid damage due to interstitial condensation. The validation results were shown in Fig. 12. For relative humidity and humidity ratio, root mean square errors were correspondingly 1.61 and 0.28 and correlation factors were 0.921 and 0.962, respectively.

5. Analysis of accuracy influence from input factors

5.1. Available climate data

5.1.1. Outdoor climate data

The classification of climatic zones in GB 50176 provides references for the classification of target cities and required meteorological parameters of simulation [39]. For instance, Fang et al. selected two to five cities in every climate zone to evaluate moisture buffering effect of

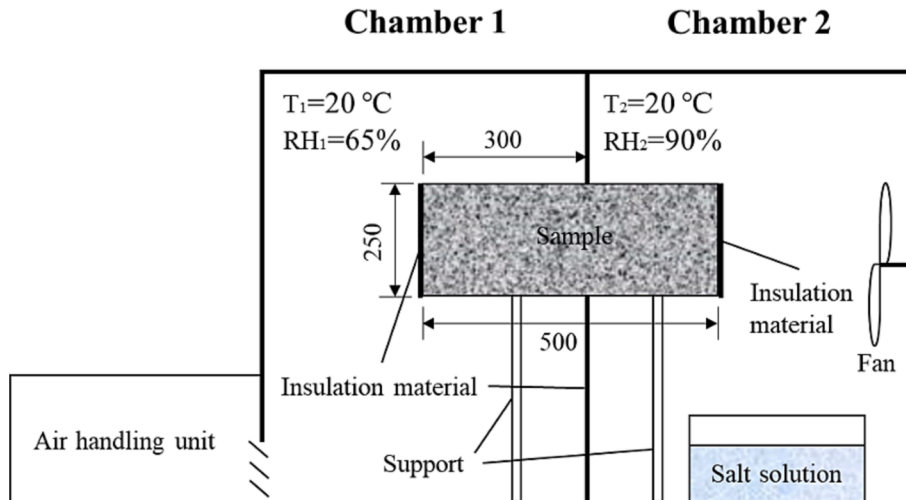


Fig. 10. Measurement apparatus to validate 2D models proposed by Qin et al. [68].

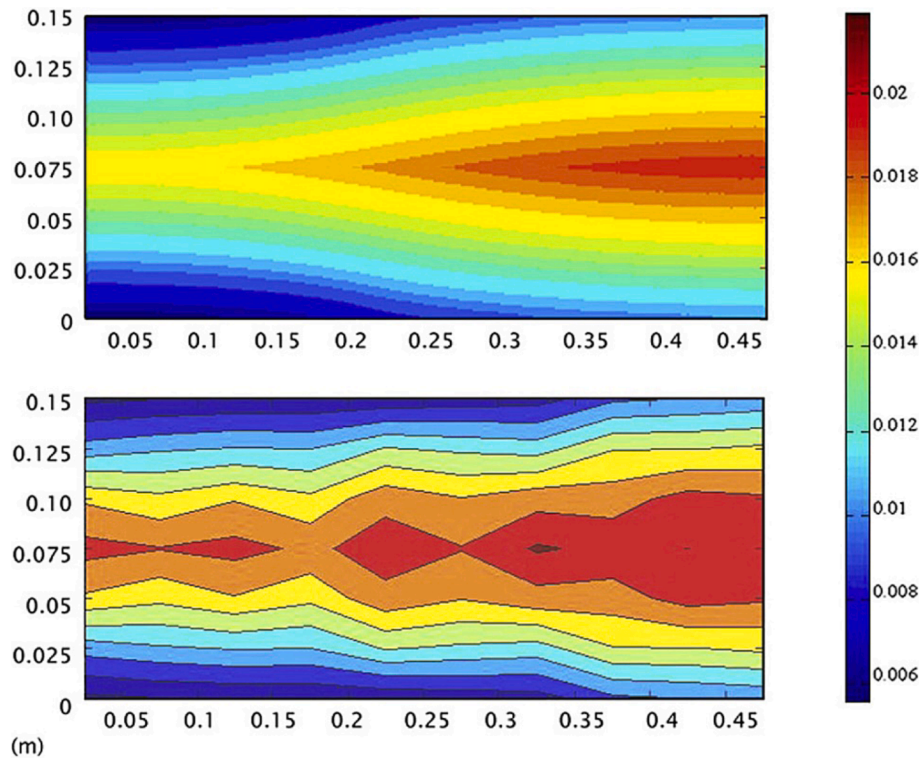


Fig. 11. Calculated moisture ratio (kg/kg) from 2D models with vapour content being moisture driving potential proposed by Qin et al. and measured data [68].

porous building materials [70]. Zhao et al. selected three to five cities in every climate zone to simulate the energy consumption [71]. However, the classification based on GB 50176 is not reasonable since the moisture load such as WDR is neglected. It would cause that some representative cities are not covered.

To access the hygrothermal performance of buildings, temperature, RH, solar radiation, wind speed and direction and rain load are basically required. However, it is time-consuming and meaningless to calculate by inputting all historic meteorological data. Therefore, representative data and reference years are applied. Two standards in China provide the reference outdoor climate data. GB 50176 simplifies temperature, solar radiation and RH to constants from extreme weather for more than 200 cities which provide exterior input for steady-state calculation referring to Glaser's method [39], while it is far from the realistic condition. JGJ/T 346 goes further, it refers to Typical Meteorological Year (TMY) to generate reference years including dry-bulb temperature, dew point temperature, solar radiation, wind speed and direction, atmosphere contradiction if possible from measured data between 1995 and 2004 [38]. Fang et al. predicted the future climate based on TMY via global climate model in Guangzhou to generate the future climate data [53]. These databases are more suitable for evaluation of thermal performance, since included parameters and generation methods are more related to thermal effect.

5.1.2. Indoor climate data

Temperature and RH are basic parameters of indoor boundary condition. There is no available database for whole year simulation. GB 50176 [39] and GB 50736 [72] provides ranges of indoor climate data to meet comfort requirement for occupants, so constants based on these standards are applied as input [52,66,73].

Tools, such as computational fluid dynamics (CFD), divide the target building into various zones to calculate the density distribution of air including heat and humidity. This method is difficult to handle with higher requirement for users' foundation and computers' operation. Additionally, the indoor climate varies with room height, which means the results from CFD method is not suitable for hygrothermal calculation

for building envelopes.

Therefore, simplified methods are referred to, with the air being quasi-steady state and well-mixed as well without changes of density, heat capacity, hydrostatic pressure. Popular methods to obtain indoor temperature and RH can be summarized into zone models, two equations can describe them.

For heat conservation equation:

$$\rho c V \frac{dT}{dt} = Q_{tran} + Q_{pro} + Q_{vent} + Q_{flow} + Q_{HVAC} \quad (27)$$

where ρ is the density of indoor air; V the volume; T the temperature; t the time; Q_{tran} the heat flow due to the solar radiation and the heat fluxes due to convection and transfer with building envelopes; Q_{pro} the heat production from occupants and equipment; Q_{vent} the heat fluxes due to ventilation; Q_{flow} the heat fluxes due to air flow in multi-zone; Q_{HVAC} heat fluxes due to operation of HVAC.

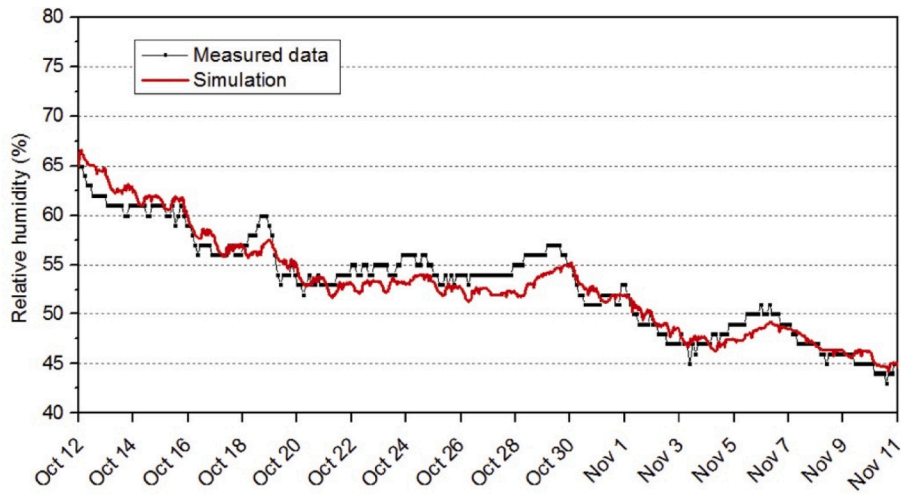
For moisture conservation equation:

$$V \frac{dv_i}{dt} = W_{tran} + W_{pro} + W_{vent} + W_{flow} + W_{HVAC} \quad (28)$$

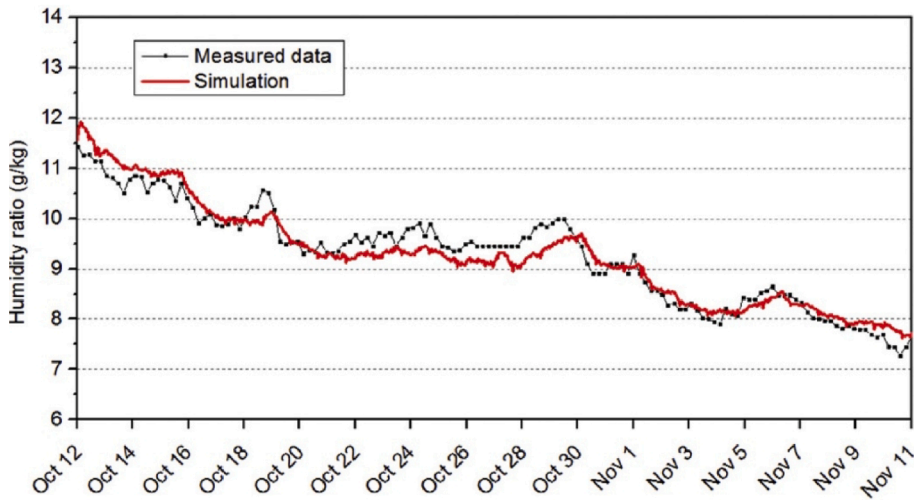
where v_i is the absolute humidity ratio of the interior air; W_{tran} the moisture fluxes due to exchange and transfer with building envelopes; W_{pro} the moisture production from occupants and equipment; W_{vent} the moisture fluxes due to ventilation; W_{flow} the moisture fluxes due to air flow among zones; W_{HVAC} moisture fluxes due to operation of HVAC.

In terms of steady-state, the left sides of above equations are equal to zero, which means the indoor climate data are constants. However, it does not consider the heat and moisture gain or loss attributed to transport, production, ventilation and operation of HVAC.

When it comes to single-zone models, the heat and moisture exchange between the indoor air and building envelopes are ignored. The sum of Q_{tran} and Q_{flow} , the sum of W_{tran} and W_{flow} from above equations are equal to zero. Chen et al. referred to single zone model [74], which means the whole building is thought of a well-mixed zone. Temperature and moisture are assumed not to vary spatially within the whole



a. RH



b. Humidity ratio

Fig. 12. Validation results between measurement and simulation from hygrothermal models with humidity ratio being moisture driving potential proposed by Zhang et al. [69].

Table 2
Summary of heat and moisture boundary condition treatment from scholars in China.

Studies	Exchange on exterior surface						Exchange on interior surface		
	Moisture		Heat				Moisture	Heat	
	Convective	WDR	Convective	Radiative	Sensible	Latent	Convective	Convective	Latent
Zhang et al. [22–24]	✓		✓	✓		✓			
Liu et al. [58]	✓		✓			✓	✓		✓
Kong et al. [15]							✓	✓	
Wang et al. [40]							✓	✓	✓
Chen et al. [9,52,66,67]	✓		✓	✓		✓	✓	✓	✓
Liu [65]	✓	✓	✓	✓	✓	✓	✓	✓	✓
Chen et al. [29]	✓		✓	✓		✓	✓	✓	✓
Fang et al. [53]	✓		✓	✓		✓	✓	✓	✓
Fang et al. [76]	✓		✓	✓	✓	✓	✓	✓	✓
Qin et al. [68]	✓	✓	✓	✓	✓	✓	✓	✓	✓
Zhang et al. [32]	✓		✓	✓		✓	✓	✓	✓
Zhang et al. [61]	✓		✓	✓		✓	✓	✓	✓

building.

Multi-zone models divide the building into a few zones, the air in independent zones is well-mixed and quasi-steady but varies from zone to zone. The total pressure is the sum of pressure in every zone via referring to Dalton’s law. Q_{tran} and W_{tran} rely on hygrothermal models. This method was used to predict the concentration of contaminants at first. These models are popular to be applied for assessment of energy consumption coupling with heat and moisture transfer in building envelopes at present. Qin et al. [75] referred to these. The indoor air is assumed as two components with dry air and water.

5.2. Treatment of boundary conditions

The terms of WDR and solar radiation are neglected on the interior surface, others are similar, so only the balance at exterior surface is shown. The summary of boundary condition treatment from scholars in China is shown in Table 2.

Moisture balance is expressed as:

$$j_e = -[\beta_e(P_{e,a} - P_{e,sur}) + (R_{wdr} - R_{runoff})] \tag{29}$$

where j_e is the moisture flow density on the exterior surface; β_e the mass exchange coefficient on the exterior surface; $P_{e,a}$ the vapour pressure of outdoor air; $P_{e,sur}$ the vapour pressure on the exterior surface; R_{wdr} WDR load; R_{runoff} the runoff rain load when the exterior surface material is saturated.

Heat balance is expressed as:

$$q_e = -[\alpha_c(T_{e,a} - T_{e,sur}) + \alpha_{e,rad}q_{e,rad} + h_v\beta_e(P_{e,a} - P_{e,sur}) + c_l(R_{wdr} - R_{runoff})(T_{wdr} - T_{sur})] \tag{30}$$

where q_e is the heat flux density on the exterior surface; α_c the convective coefficient; $T_{e,a}$ the temperature of outdoor air; $T_{e,sur}$ the temperature on the exterior surface; $\alpha_{e,rad}$ absorptivity of solar radiation; $q_{e,rad}$ the solar radiation; h_v the latent heat of evaporation; c_l the specific heat of liquid water; T_{wdr} the temperature of WDR; T_{sur} the temperature of the exterior surface.

5.3. Hygric material properties

Moisture in building materials can be present in three phases with vapour, water and ice under different environment condition. Since physical states are difficult to be separately measured, functions with a few parameters of total water content by relative humidity (RH) are used to describe the capability of building materials to store moisture. e.g. in

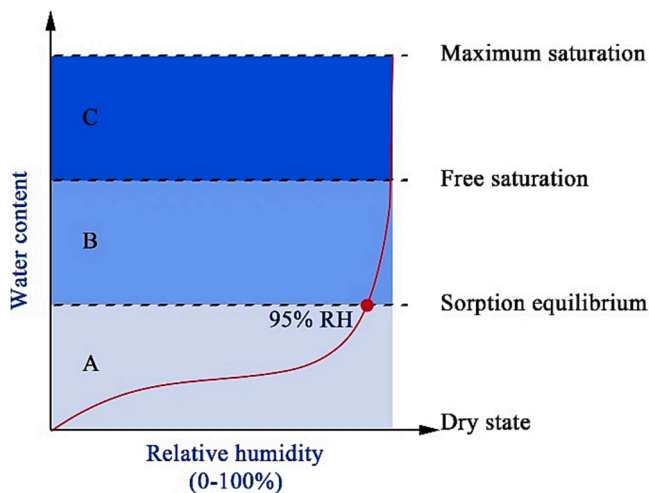


Fig. 13. Total water content defined to 3 sections referred to Hartwig M. Künzel corresponding to different test standards and methods [57].

China, Oswin [77], Henderson [78], Caurie [79], Guggenheim-Anderson-de Boer (GAB) [80], Peleg [81], were popularly applied as fitting formulas [82,83]. A new formula with fewer parameters than Peleg’s was proposed by Feng et al. for common porous building materials [84]. Three moisture ranges to show total water content from A to C are according to literature [57], shown in Fig. 13.

Range A is described by the sorption isotherm at RH below 95 %. There is equilibrium of moisture sorption between materials and ambient moist air. Range B is the capillary water region from sorption moisture at 95 % RH to free water saturation with forces of capillary pressure or suction stress. This region occurs when building materials are in contact with liquid water or super-hygroscopic moisture substances. There is also equilibrium of water content before capillary pressure or suction stress decreases to zero. Range C is the supersaturated region, the ambient RH is 100 %. This is the region for hydrophobic insulation materials when condensation occurs. Independent of the amount of condensate, RH at the condensation plane remains at 100 % as long as liquid water is present. This means, there is no definable equilibrium between the water content of the material and the ambient humidity.

There is no database of hygric properties in China. Chinese standard GB/T 20312 similar to ISO 12571 recommends the desiccator method to measure range A at 23°C [85]. Currently, there is no Chinese standard of measurement methods for range B. A pressure plate test is applied to test range B to interpolate the moisture retention curve up to the free water saturation [86]. A new standard to determine water absorption properties is T/CECS 743 [87]. Compared with ASTM C1749, the standard specifies a larger range of test temperature and RH. The data processing is nonlinear. In addition, it provides an equation to calculate the water absorption coefficient of the same sample under different temperature, shown in Table 3.

In range A and B, autoclaved aerated concrete, calcium silicate board and ceramic brick were tested at the range of 10 – 40°C in literature [88], which the result shows that temperature effect can be disregarded. However, anisotropy was distinct in both ranges when sandstones were tested in literature [89]. Additionally, hysteresis effect of range A is characteristic for bio-based materials such as wood, which was validated by Zhang et al. [22–24,90].

GB/T 17146 similar to ISO 12572 provides wet-dry cup method to measure vapour permeability at 23°C [91]. There is no Chinese standard for the measurement of liquid permeability. It can be measured by the method of water head or transformed by moisture diffusivity. The test of moisture diffusivity relies on recordings of transient moisture distributions during the water absorption test with subsequent diffusivity determination by reverse calculation based on Boltzmann transformation. Non-destructive methods include γ -ray, X-ray, nuclear magnetic resonance, etc.. To simplify the apparatus and procedure of data

Table 3

Methods and corresponding standards in China and abroad to measure hygric properties including both storage and transport at different water content defined by Hartwig M. Künzel.

Properties	Methods	Standards	Features
Storage	Sorption isotherm	Desiccator	GB/T 20312 12571 [85]
	Moisture retention curve	Partial immersion	T/CECS 743 [87]
Transport	Vapour permeability	Wet-dry cup	GB/T 17146 12572 [91]
	Liquid permeability		

processing, the ruler and the multi-step methods based on modification of capillary absorption test, and the Kießl-Künzel method based on standard capillary absorption test and evaluation are applied [92].

6. Discussion

6.1. Model application for different purposes in China

6.1.1. Condensation and mould growth risks

Temperate environment, high moisture load, suitable substrate and adequate exposure time may induce mould growth. Once the vapour pressure reaches the saturated vapour pressure (RH is 100 %), vapour condenses to liquid water. White-box hygrothermal models can be applied to evaluate the risks of these problems.

Guo et al. [93] applied the white-box hygrothermal models with moisture content being the driving potential to predict the likelihood of condensation in building envelopes. They assumed that there was no liquid water transfer. Both outdoor and indoor climate data were constants. Target constructions were composed by 20 mm plasterboard, 100 mm glass wool and 20 mm brick masonry from outdoor to indoor. Their method is similar to Glaser’s method, which GB 50176 referred to, but the investigated constructions appear to be rather simple and a bit far from reality.

Chen et al. [94] applied their white-box hygrothermal models with RH being the driving potential to predict the risk of mould growth in 104 cities located in the south of China. Outdoor climate data were taken from TMY files, while indoor climate data were constants. Target constructions were 240 mm red brick with 20 mm lime-cement mortar on both sides. They assumed that there was a risk of mould growth, if both the RH and temperature were simultaneously higher than 80 % and 0°C. The index of risk is expressed as:

$$S_{RH80} = \sum_1^n (RH_n - RH_0)(T_n - T_0) \tag{31}$$

where S_{RH80} is the index of mould growth risk; RH_0 80 %; T_0 0°C; n the number of data; RH_n the RH of the n th datum higher than 80 %; T_n the temperature of the n th datum higher than 0°C. The result shows that the risk of mould growth in cities located in the southeast was the highest. According to literature [95] and [96], bio-based materials are more prone to mould growth than mineral materials at higher relative humidity and temperature. However, Eq. (31) overestimate the risk of mould growth even for these materials.

6.1.2. Hygric effect on thermal performance

White-box hygrothermal models can predict the temperature, heat flux density, moisture distribution and total moisture content, etc. of building materials in building envelopes. Then, the total thermal performance of wet building materials is calculated.

Chen et al. [97] applied white-box hygrothermal models with RH being the moisture driving potential to correct the average heat transfer

coefficient with moisture influence of load-bearing structure via Eq. (32),

$$q_{cr} = \frac{q - q'}{q} \tag{32}$$

where q_{cr} is correction rate; q' the heat flux density without moisture load. Typical cities were classified into three humidity zones via wet-bulb temperature. Outdoor climate data including temperature and RH were hourly data from the hottest and the coldest month and indoor boundary condition were constants. Target constructions followed standards in different climatic zones. The comparison results are shown in Table 4. However, the heat transfer coefficient is relevant with both heat flux and temperature. Therefore, the simplification in Eq. (32) might lead to inaccurate calculation results.

Kong et al. [98] applied their white-box hygrothermal models with RH being the moisture driving potential to calculate the moisture content of separate building materials in building envelopes. Outdoor climate data were monthly average temperature and RH from 1991 to 2000 in Harbin located in severe cold zone. Indoor climate data were constants. Target construction was exterior insulation system by following the construction standard in severe cold and cold zones. They assumed dry building materials and moisture in envelope were linked to each other by half series and half parallel connection, while the moisture is not evenly distributed in building envelopes and materials. The ten-year calculation results show that the total heat transfer coefficient in winter was dramatically decreasing. The average specific heat, thermal storage coefficient and thermal inertia index of insulation material were considerably increasing. In fact, the specific heat and thermal storage coefficient of water are higher than insulation materials, results might be unreasonable.

6.1.3. HVAC load and indoor climate

In Eq. (27) and (28), white-box hygrothermal models are applied to calculate the Q_{tran} and W_{tran} through building envelopes. Normally, Q_{pro} , Q_{vent} , Q_{flow} , W_{pro} , W_{vent} , W_{flow} are confirmed by reference values or empirical formulas. If indoor temperature and RH are confirmed, such as being maintained under fixed values, the HVAC load is predicted. If HVAC load is confirmed, indoor temperature and RH are predicted.

Chen et al. [33], Fang et al. [53,76], Liu et al. [52,66] assumed the sum of Q_{pro} , Q_{vent} , Q_{flow} , W_{pro} , W_{vent} , W_{flow} and the left sides were equal to zero to calculate the HVAC load for cities in the south China, which means the indoor climate data were constants and the indoor climate was totally controlled by HVAC system. Target constructions were typical modern constructions. White-box hygrothermal models from Fang et al. [76] applied capillary pressure being driving potential, and Chen et al. [33] and Liu et al. [52] applied RH being driving potential. Outdoor climate data were from TMY dataset, precipitation data in Fang et al.’s literature were added via the method in ISO 15927-3 [100]. The results show that the heating and cooling load without precipitation via white-box hygrothermal models was underestimated compared with

Table 4
Correction rate of heat transfer coefficient from simplified models without considering temperature change in article [97] by Chen et al.

Humidity zones	Cities	Aerated concrete		Concrete		Clay brick	
		Summer	Winter	Summer	Winter	Summer	Winter
Wet	Hefei	17.2	1.4	7.4	-0.6	11.3	0.9
	Fuzhou	11.9	-8.1	5.2	-7.7	7.9	-1.9
Moderate	Changchun	14.0	1.9	9.5	0.6	13.4	0.8
	Xi'an	11.9	1.3	8.0	0.9	8.1	1.1
	Hangzhou	15.3	-1.1	7.0	-1.8	13.0	0.4
	Guangzhou	16.7	-24.0	7.3	-8.4	9.6	-9.3
	Guiyang	31.0	-1.1	22.9	0.8	25.1	-0.2
Dry	Hohhot	-5.0	1.8	-10.2	0.5	-2.5	0.8
	Lanzhou	8.6	3.4	-4.9	0.6	-8.2	0.9
	Kunming	-4.2	8.0	-1.2	5.4	-3.2	4.0

estimation via heat models, while the cooling load with WDR was overestimated too much. Even though these methods simplified a lot, it shows the influence of moisture load especially rain drops on evaluation of HVAC load is distinct. Liu et al. optimized the insulation thickness in literature via the correlation between economic model and HVAC load [66]. The results were shown in Table 5.

Kong et al. [20] applied white-box hygrothermal models, with moisture content being moisture driving potential, and zone models in single room to predict indoor temperature and RH. Q_{flow} , W_{flow} were assumed to be zero, which means there was no airflow between two rooms. The outdoor climate data were one-year daily average values of temperature and RH and the indoor climate data were constants. The heat and moisture transfer were assumed in a north-oriented wall composed with typical exterior insulation system in Harbin in cold zone with 100 mm insulation. Qin et al. [75] applied white-box hygrothermal models, with vapour pcontent being moisture driving potential, and zone models to evaluate the indoor temperature and RH in a residential building in Guangzhou. Outdoor boundary condition were one-week hourly data including temperature and RH. Target construction was neither modern nor historic constructions in China.

6.2. Suggested models

The driving potentials or driving forces for moisture transfer are different for vapour and liquid flow. For vapour diffusion the physical driving force is the partial vapour pressure. For capillary flow, it is the capillary pressure also called suction pressure. Alternatively, the more common parameter RH can be used, because there is a direct relationship between capillary pressure and RH called the Kelvin equation. Models considering only one driving force, e.g. vapour flow have their own application situations and limitations. Since the driving forces for vapour and liquid flow may be opposed to each other, neglecting one of them may severely reduce the range of model application. This would become evident in winter when the hygroscopic building materials start to absorb moisture from the dry state, the indoor vapor pressure is higher than the outdoor air under the operation of heating system, while the outdoor RH is higher than the indoor or even WDR penetrates. Therefore, independent driving potentials are required. Physical process and real condition should be considered. Water content or volumetric moisture ratio are non-continuous at interfaces when being applied to multi-layer building envelopes. The following parameters and driving potentials are suggested for models in different situations:

(1) Moisture loads acting on the building envelope include: vapour exchange between outdoor or indoor air, WDR and groundwater. If liquid water transfer can be excluded, the last two terms are ignored, as e.g. in Glaser's method [101] in GB 50176 [39].

(2) If both hysteresis-effect and temperature-dependency are not negligible especially for bio-based materials, models considering temperature-dependent hysteresis-effect are suggested for moisture buffering effect of wood-based interior finish, as e.g. models proposed by Zhang et al in [22–24].

(3) In climatic zones with wintertime temperatures below 0 °C, ice formation may occur. Therefore, the enthalpy of freeze and thaw should

Table 5
Optimum results of insulation thickness from economic model and simplified zone models applied by Liu et al. [66].

City	Material	Thickness (m)	
		Heat models	Hygrothermal models
Changsha	Expanded polystyrene	0.100	0.105
	Extruded polystyrene	0.065	0.069
Chengdu	Expanded polystyrene	0.091	0.097
	Extruded polystyrene	0.059	0.064
Shaoguan	Expanded polystyrene	0.078	0.081
	Extruded polystyrene	0.051	0.053

be considered in the heat equation. Also, the thermal conductivity of ice more than three times higher, than that of liquid water. Ice in porous materials may also block capillary flow [102]. Thus, models considering ice formation and its effect on hygrothermal transport parameters are suitable to be applied for the climatic zones in the north of China, as e.g. models proposed by Kong et al. in [15].

(4) Water absorption and drying process by evaporation are alternating phenomena in façade materials. If the amount of water caused by WDR penetration is higher than the amount of evaporated water, moisture accumulation will occur. These effects can only be captured by models that account for liquid transport as well as vapour diffusion, as e.g. models proposed by Fang et al in [53].

(5) The volumetric moisture content is non-continuous over the interface of materials from different layers. If the envelope is single-layer without interface, models with volumetric moisture ratio being the driving potential are suitable, as e.g. models from Philip and De Vries [103].

(6) Airflow driven by buoyancy, wind or mechanical ventilation pressure differentials may cause interstitial condensation at joints or thermal bridges. If liquid water transfer and ice formation is neglected, 2D models proposed by Qin et al. can be applied to calculate thermal bridge effects without WDR penetration and interstitial condensation, since only vapour content is reflected, as e.g. models in [68].

7. Conclusions and future perspectives

The high moisture loads in the south where most people live in shows that it is essential to propose hygrothermal white-box models to predict heat and moisture transfer in building envelopes. Models proposed by Chinese researchers target on specific cases, which is meaningful to further understand heat and moisture transfer in building envelopes. Based on assumptions, the reliability and accuracy of models vary from climate features and building components in China. These models are complicated and practitioners need to judge the physical phenomena and limitations. For instance, temperature-dependent hysteresis-effect is not distinct in most construction materials and the desorption isotherm is not available for most materials. Models with only capillary pressure being driving potential cannot calculate the drying process. 2D models require users to judge boundary conditions and angle-dependent properties. Furthermore, most models in China are not available for the public, although a few are developed to be personal tools [104,105].

In fact, both accuracy and availability of models or tools should be included. Although all features cannot be covered, they would be reliable to analyze common practical cases. In China, GB 50176 highlights limits of moisture content in different insulation materials. It is necessary to apply hygrothermal white-box models or tools for construction design to meet the standard requirements, and models should be easily handled by engineers.

Therefore, the universal models can be 1D transient and focus on separate driving potentials of vapor and liquid water transfer when it comes to higher indoor RH or vapor pressure, but temperature-dependent hysteresis-effect and thermodiffusion can be neglected. To obtain the reliable output, suitable representative outdoor climate data, such as moisture reference years or hygrothermal reference years including precipitation, are better to be selected [43,106–108]. Indoor climate data deriving from occupants' behavior are suggested to be applied as indoor climate input.

CRedit authorship contribution statement

Tingting Zhang: Funding acquisition, Methodology, Resources, Visualization, Writing – original draft. **Hartwig M. Künzle:** Conceptualization, Supervision, Visualization, Writing – review & editing. **Daniel Zirkelbach:** Investigation, Supervision, Writing – review & editing. **Mingfang Tang:** Investigation, Visualization. **Kehua Li:** Investigation, Validation. **Tobias Schöner:** Investigation. **Jing Ren:** Investigation.

Declaration of competing interest

The authors declare that they have no known competing financial interests or personal relationships that could have appeared to influence the work reported in this paper.

Data availability

Data will be made available on request.

Acknowledgements

Authors thank for financial support from China Scholarship Council (CSC) for Tingting Zhang during the stay at Fraunhofer institute for Building Physics (No. 202106050110). Authors also thank the invaluable help from Geraldine F. Ajero, Qiujia Lai, Jinzhong Fang, Mengli Zhou and Chuanqun Zhang.

References

- [1] B. Lin, Z. Wang, Y. Liu, Y. Zhu, Q. Ouyang, Investigation of winter indoor thermal environment and heating demand of urban residential buildings in China's hot summer - cold winter climate region, *Build. Environ.* 101 (2016) 9–18, <https://doi.org/10.1016/j.buildenv.2016.02.022>.
- [2] MOHURD, JGJ 26, Design standard for energy efficiency of residential buildings in severe cold and cold zones, 2010. (in Chinese).
- [3] MOHURD, JGJ 134, Design standard for energy efficiency of residential buildings in hot summer and cold winter zone, 2010. (in Chinese).
- [4] MOHURD, JGJ 75, Design standard for energy efficiency of residential buildings in hot summer and warm winter zone 2012. (in Chinese).
- [5] MOHURD, JGJ 475, Standard for design of energy efficiency of residential buildings in moderate climate zone, 2019. (in Chinese).
- [6] Y. Wang, J. Huang, D. Wang, Y. Liu, J. Liu, Experimental study on hygrothermal characteristics of coral sand aggregate concrete, *Constr. Build. Mater.* 230 (2020) 117034, <https://doi.org/10.1016/j.conbuildmat.2019.117034>.
- [7] J. Wang, Z. Yan, L. Sun, Field test and analysis of indoor thermal environment in the earthen heritage site museum, *Build. Sci.* 26 (2010) 27–31 (in Chinese). <https://doi.org/10.13614/j.cnki.11-1962/tu.2010.08.008>.
- [8] J. Zhu, P. Nie, L. Tong, X. Zhao, C. Xing, Thermal response characteristics of cliff-side cave dwellings in west area of He'nan under extreme climate condition, *Build. Sci.* 33 (2017) 76–89 (in Chinese). <https://doi.org/10.13614/j.cnki.11-1962/tu.2017.12.12>.
- [9] W. Dong, Y. Chen, Y. Bao, A. Fang, A validation of dynamic hygrothermal model with coupled heat and moisture transfer in porous building materials and envelopes, *J. Build. Eng.* 32 (2020) 101484, <https://doi.org/10.1016/j.jobbe.2020.101484>.
- [10] Z. Xie, Q. Wei, T. Long, The influence of environment and humidity on the shuijingfang site, *Sci. Conserv. Archaeol.* 17 (2004) 46–49 (in Chinese). <https://doi.org/10.16334/j.cnki.cn31-1652/k.2005.03.011>.
- [11] Y. Li, H. Xie, J. Wang, X. Shi, Comparative study of isothermal sorption properties of traditional blue bricks in historic building, *J. Build. Mater.* 17 (2014) 1092–1095 (in Chinese). <https://doi.org/10.3969/j.issn.1007-9629.2014.06.027>.
- [12] MOHURD, 12J201, The construction of flat roof, 2012. (in Chinese).
- [13] MOHURD, JGJ/T 261, Technical specification for interior thermal insulation on external walls, 2011. (in Chinese).
- [14] MOHURD, JGJ 144, Technical standard for external thermal insulation on walls, 2019. (in Chinese).
- [15] F. Kong, Q. Zhang, Effect of heat and mass coupled transfer combined with freezing process on building exterior envelope, *Energy Build.* 62 (2013) 486–495, <https://doi.org/10.1016/j.enbuild.2013.03.012>.
- [16] M. Tang, J. Fang, J. Li, D. Wang, P. Song, Investigation of condensation on ground of rural residence in Chongqing, *J. Civ. Environ. Eng.* 38 (2016) 123–128 (in Chinese).
- [17] W. Liu, C. Huang, Y. Hu, Z. Zou, L. Shen, J. Sundell, Associations of building characteristics and lifestyle behaviors with home dampness-related exposures in Shanghai dwellings, *Build. Environ.* 88 (2015) 106–115, <https://doi.org/10.1016/j.buildenv.2014.10.028>.
- [18] C. Zhang, M. Tang, C. Feng, Study on the internal condensation of compound insulating metal roof, *Build. Sci.* 37 (2021) 60–65 (in Chinese). <https://doi.org/10.13614/j.cnki.11-1962/tu.2021.04.08>.
- [19] K. Zou, S. Li, Analysis of condensation characteristics and anti-condensation measures of external thermal insulation wall in hot summer and cold winter areas, *J. Southeast Univ.* 48 (2018) 654–661 (in Chinese).
- [20] F. Kong, H. Wang, Effect of envelope heat and mass coupled transfer on indoor environment, *J. Therm. Sci. Technol. (dalian, China)* 9 (2010) 212–217 (in Chinese).
- [21] WUFI. <https://wufi.de/en>.
- [22] X. Zhang, H.M. Künnel, W. Zillig, C. Mitterer, X. Zhang, A fickian model for temperature-dependent sorption hysteresis in hygrothermal modeling of wood materials, *Int. J. Heat Mass Transfer* 100 (2016) 58–64, <https://doi.org/10.1016/j.ijheatmasstransfer.2016.04.057>.
- [23] X. Zhang, W. Zillig, H.M. Künnel, C. Mitterer, X. Zhang, Combined effects of sorption hysteresis and its temperature dependency on wood materials and building enclosures-part I: measurements for model validation, *Build. Environ.* 106 (2016) 143–154, <https://doi.org/10.1016/j.buildenv.2016.06.025>.
- [24] X. Zhang, W. Zillig, H.M. Künnel, C. Mitterer, X. Zhang, Combined effects of sorption hysteresis and its temperature dependency on wood materials and building enclosures-part II: hygrothermal modeling, *Build. Environ.* 106 (2016) 181–195, <https://doi.org/10.1016/j.buildenv.2016.06.033>.
- [25] Y. Chen, Z. Chen, The simultaneous heat and moisture transfer equations of porous building envelope and their linearization, *J. Basic Sci. Eng.* 5 (1997) 167–171 (in Chinese).
- [26] CNKI. <https://www.cnki.net/>.
- [27] Wanfang. <http://www.wanfangdata.com.cn/index.html>.
- [28] CQVIP. <http://www.cqvip.com/>.
- [29] Y. Chen, Z. Chen, Frequency domain method to solve linear simultaneous heat and moisture transfer equations, *J. Basic Sci. Eng.* 6 (1998) 167–171 (in Chinese).
- [30] X. Guo, Y. Chen, Analysis of the hygrothermal performance of multilayer wall exposed to hot and humid climate, *J. Hunan Univ.* 35 (2008) 1–4 (in Chinese).
- [31] X. Guo, Y. Chen, L. Zhang, Analysis of the hygrothermal performance of a new timber structure wall, *J. Hunan Univ.* 36 (2009) 18–21 (in Chinese).
- [32] L. Zhang, Y. Chen, Study on the effect of solar radiation on the hygrothermal properties of multi-layer walls in the south of China, *Build. Sci.* 26 (2010) 332–336 (in Chinese). <https://doi.org/10.13614/j.cnki.11-1962/tu.2010.10.063>.
- [33] Y. Chen, Y. Bao, W. Dong, A. Fang, Effect of coupled heat and moisture transfer on building energy consumption simulation along the Yangtze river basin, *J. Huazhong Univ. Sci. Technol.* 48 (2020) 72–77 (in Chinese). <https://doi.org/10.13245/j.hust.200212>.
- [34] H. Zhou, M. Qian, J. Feng, L. Sun, *Manual of Thermal Properties and Data for Building Materials*, China Architecture Publishing, Beijing, 2010 (in Chinese).
- [35] Q. Chen, *Building Thermophysics*, Xi'an Jiaotong University Press, Xi'an, 1991 (in Chinese).
- [36] B. Wang, *Heat and Mass Transfer*, Science Press, Beijing, 1982 (in Chinese).
- [37] B. Wang, *Heat and Mass Transfer*, Science Press, Beijing, 2015 (in Chinese).
- [38] MOHURD, JGJ/T 346, Standard for weather data of building energy efficiency, 2015. (in Chinese).
- [39] MOHURD, GB 50176, Thermal design code for civil building, 2016. (in Chinese).
- [40] X. Wang, X. Jin, Y. Yin, X. Wang, X. Shi, X. Zhou, Study on non-isothermal moisture transfer characteristics of hygroscopic building materials: From parameter characterization to model analysis, *Energy* 212 (2020) 118788, <https://doi.org/10.1016/j.energy.2020.118788>.
- [41] Q. Pei, Study on identification method for the dynamic moisture performance of building envelopes, *Hunan University, Hunan*, (in Chinese).
- [42] CMA. <http://data.cma.cn/>.
- [43] S. Cornick, R. Djebbar, W.A. Dalglish, Selecting moisture reference years using a moisture index approach, *Build. Environ.* 38 (2003) 1367–1379, [https://doi.org/10.1016/S0360-1323\(03\)00139-2](https://doi.org/10.1016/S0360-1323(03)00139-2).
- [44] T. Qian, H. Zhang, Assessment of long-term and extreme exposure to wind-driven rain for buildings in various regions of China, *Build. Environ.* 189 (2021) 107524, <https://doi.org/10.1016/j.buildenv.2020.107524>.
- [45] H. Zhang, H. Yoshino, Analysis of indoor humidity environment in Chinese residential buildings, *Build. Environ.* 45 (2010).
- [46] H. Zhang, H. Yoshino, S. Murakami, K. Bogaki, T. Tanaka, S.-I. Akabayashi, K. Abe, Analyses of indoor humidity environment in nationality residential houses of Japan, *AIJ J. Technol. Des.* 15 (2009) 453–457, <https://doi.org/10.3130/aijt.15.453>.
- [47] CEN, EN 15026, Hygrothermal performance of building components and building elements - Assessment of moisture transfer by numerical simulation, 2007.
- [48] C.E. Hagento, HAMSTAD-Final Report: Methodology of HAM-Modeling, Report R-02:8, 2002.
- [49] P. Talukdar, S.O. Olutmayin, O.F. Osanyintola, C.J. Simonson, An experimental data set for benchmarking 1-D, transient heat and moisture transfer models of hygroscopic building materials. Part I: Experimental facility and material property data, *Int. J. Heat Mass Transfer* 50 (2007) 4527–4539, <https://doi.org/10.1016/j.ijheatmasstransfer.2007.03.026>.
- [50] P. Talukdar, S.O. Olutmayin, O.F. Osanyintola, C.J. Simonson, An experimental data set for benchmarking 1-D, transient heat and moisture transfer models of hygroscopic building materials. Part II: Experimental, numerical and analytical data, *Int. J. Heat Mass Transfer* 50 (2007) 4915–4926, <https://doi.org/10.1016/j.ijheatmasstransfer.2007.03.025>.
- [51] X. Liu, G. Chen, Y. Chen, Modeling of the transient heat, air and moisture transfer in building walls, *J. Hunan Univ.* 43 (2016) 152–156 (in Chinese).
- [52] X. Liu, Y. Chen, H. Ge, P. Fazio, G. Chen, Numerical investigation for thermal performance of exterior walls of residential buildings with moisture transfer in hot summer and cold winter zone of China, *Energy Build.* 93 (2015) 259–268, <https://doi.org/10.1016/j.enbuild.2015.02.016>.
- [53] A. Fang, Y. Chen, L. Wu, Transient simulation of coupled heat and moisture transfer through multi-layer walls exposed to future climate in the hot and humid southern China area, *Sustainable Cities Soc.* 52 (2020) 101812, <https://doi.org/10.1016/j.scs.2019.101812>.
- [54] H.E. Huerto-Cardenas, F. Leonforte, N. Aste, C.D. Pero, G. Evola, V. Costanzo, E. Lucchi, Validation of dynamic hygrothermal simulation models for historical buildings: state of the art, research challenges and recommendations, *Build. Environ.* 180 (2020) 107081, <https://doi.org/10.1016/j.buildenv.2020.107081>.

- [55] H. Janssen, Thermal diffusion of water vapour in porous materials: a critical review, International conference on durability of building materials and components, Porto, 2011.
- [56] ASHRAE handbook, Peachtree Corners, 2021.
- [57] H.M. Künzle, *One and two-dimensional calculation of the simultaneous heat and moisture transport in building components, using simple parameters*, Fraunhofer Institute for Building Physics, 1995.
- [58] Y. Liu, Y. Wang, D. Wang, J. Liu, Effect of moisture transfer on internal surface temperature, *Energy Build.* 60 (2013) 83–91, <https://doi.org/10.1016/j.enbuild.2013.01.019>.
- [59] H. Hens, Modeling the heat, air, and moisture response of building envelopes: what material properties are needed, how trustful are the predictions? *J. ASTM Int.* 4 (2007) <https://doi.org/10.1520/JAI100460>.
- [60] A.C. Dilley, On the computer calculation of vapor pressure and specific humidity gradients from psychrometric data, *J. Appl. Meteorol.* 7 (1968) 717–719, [https://doi.org/10.1175/1520-0450\(1968\)0072.0.CO;2](https://doi.org/10.1175/1520-0450(1968)0072.0.CO;2).
- [61] H. Zhang, H. Yoshino, A. Iwamae, K. Hasegawa, Investigating simultaneous transport of heat and moisture in hygroscopic materials by a semi-conjugate CFD-coupled approach, *Build. Environ.* 90 (2015) 125–135, <https://doi.org/10.1016/j.buildenv.2015.03.028>.
- [62] L. Sun, C. Feng, Y. Cui, Influence of temperature and moisture content on the thermal conductivity of building materials, *J. Civ. Environ. Eng.* 39 (2017) 123–128 (in Chinese). <https://doi.org/10.11835/j.issn.1674-4764.2017.06.017>.
- [63] X. Wang, X. Jin, Y. Yin, X. Shi, X. Zhou, A transient heat and moisture transfer model for building materials based on phase change criterion under isothermal and non-isothermal conditions, *Energy* 224 (2021) 120112, <https://doi.org/10.1016/j.energy.2021.120112>.
- [64] M. Qin, J. Yang, Evaluation of different thermal models in EnergyPlus for calculating moisture effects on building energy consumption in different climate conditions, *Build. Simul.* 9 (2016) 15–25, <https://doi.org/10.1016/j.proeng.2015.09.194>.
- [65] X. Liu, *Investigation of the coupled heat, air and moisture transport in building walls in hot summer and cold winter zone*, Hunan University, Hunan, 2015 (in Chinese).
- [66] X. Liu, Y. Chen, H. Ge, P. Fazio, G. Chen, X. Guo, Determination of optimum insulation thickness for building walls with moisture transfer in hot summer and cold winter zone of China, *Energy Build.* 109 (2015) 361–368, <https://doi.org/10.1016/j.proeng.2015.09.072>.
- [67] Y. Bao, Y. Chen, X. Liu, W. Dong, A. Fang, Simulation model of coupled heat and moisture transfer in porous building elements and its verification, *Build. Sci.* 34 (2018) 66–75 (in Chinese). <https://doi.org/10.13614/j.cnki.11-1962/tu.2018.1.0.09>.
- [68] M. Qin, A. Ait-Mokhtar, R. Belarbi, Two-dimensional hygrothermal transfer in porous building materials, *Appl. Therm. Eng.* 30 (2010) 2555–2562, <https://doi.org/10.1016/j.applthermaleng.2010.07.006>.
- [69] L. Shi, H. Zhang, Z. Li, X. Man, Y. Wu, C. Zheng, J. Liu, Analysis of moisture buffering effect of straw-based board in civil defence shelters by field measurements and numerical simulations, *Build. Environ.* 143 (2018) 366–377, <https://doi.org/10.1016/j.buildenv.2018.07.018>.
- [70] J. Fang, H. Zhang, P. Ren, B.-J. He, M. Tang, C. Feng, Influence of climates and materials on the moisture buffering in office buildings: a comprehensive numerical study in China, *Environ. Sci. Pollut. Res.* 29 (2021) 1–18, <https://doi.org/10.1007/s11356-021-16684-3>.
- [71] M. Zhao, H.M. Künzle, F. Antretter, Parameters influencing the energy performance of residential buildings in different Chinese climate zones, *Energy Build.* 96 (2015) 64–75, <https://doi.org/10.1016/j.enbuild.2015.03.007>.
- [72] MOHURD, GB 50736, Design code for heating ventilation and air conditioning of civil buildings, 2012. (in Chinese).
- [73] S. Zhao, E.D. Angelis, Reducing mould risk during the building design stage: case studies in south-East China, *J. Constr. Dev. Countries* 25 (2020) 1–20, <https://doi.org/10.21315/jcdc2020.25.1.1>.
- [74] Y. Chen, Z. Chen, Simulation of indoor environment and space cooling load considering moisture absorption and desorption in buildings, *J. Hunan Univ.* 25 (1998) 70–107 (in Chinese).
- [75] M. Qin, G. Walton, R. Belarbi, F. Allard, Simulation of whole building coupled hygrothermal-airflow transfer in different climates, *Energy Convers. Manage.* 52 (2011) 1470–1478, <https://doi.org/10.1016/j.enconman.2010.10.010>.
- [76] A. Fang, Y. Chen, L. Wu, Modeling and numerical investigation for hygrothermal behavior of porous building envelope subjected to the wind driven rain, *Energy Build.* 231 (2021) 110572, <https://doi.org/10.1016/j.enbuild.2020.110572>.
- [77] C.R. Oswin, The kinetics of package life. III. The isotherm, *J. Soc. Chem. Ind.* 65 (1946) 419–421.
- [78] S.M. Henderson, A basic concept of equilibrium moisture, *Agric. Eng.* 1952.
- [79] M. Laurie, A new model equation for predicting safe storage moisture level for optimum stability of dehydrated foods, *Int. J. Food Sci. Technol.* 5 (2007) 301–307.
- [80] R.B. Anderson, Modifications of the Brunauer, Emmett and Teller Equation1, *J. Am. Chem. Soc.* 68 (1948) 686–691, <https://doi.org/10.1021/ja01185a017>.
- [81] M. Peleg, Assessment of a semi-empirical four parameter general model for sigmoid moisture sorption isotherms, *J. Food Process Eng.* 16 (2010) 21–37, <https://doi.org/10.1111/j.1745-4530.1993.tb00160.x>.
- [82] W. Zhang, Y. Gao, X. Lin, Study on static hygroscopic properties of porous building materials, *Build. Sci.* 35 (2019) 60–65 (in Chinese). <https://doi.org/10.13614/j.cnki.11-1962/tu.2019.04.09>.
- [83] T. Zhang, M. Ran, J. Ren, B. Wang, J. Xu, Measurement and optimal fitting of isothermal moisture absorption curve for fiberglass, *J. Huaqiao Univ Nat. Sci.* 39 (2018) 205–209 (in Chinese).
- [84] C. Feng, Study on the test methods for the hygric properties of porous building materials, South China University of Technology, Guangzhou, 2014 (in Chinese).
- [85] S. Administration, GB/T 20312, Hygrothermal performance of building materials and products - Determination of hygroscopic sorption properties, 2006. (in Chinese).
- [86] ISO 11274, Soil quality - Determination of the water-retention characteristic - Laboratory method, 2019.
- [87] CECS, T/CECS 743, Partial immersion test method for the water absorption properties of building materials and products, 2020. (in Chinese).
- [88] C. Feng, H. Janssen, Hygric properties of porous building materials (II): analysis of temperature influence, *Build. Environ.* 99 (2016) 107–118, <https://doi.org/10.1016/j.buildenv.2016.01.016>.
- [89] J. Zhao, R. Plagge, Characterization of hygrothermal properties of sandstones - impact of anisotropy on their thermal and moisture behaviors, *Energy Build.* 107 (2015) 479–494, <https://doi.org/10.1016/j.enbuild.2015.08.033>.
- [90] X. Zhang, W. Zillig, H.M. Künzle, X. Zhang, C. Mitterer, Evaluation of moisture sorption models and modified Mualem model for prediction of desorption isotherm for wood materials, *Build. Environ.* 92 (2015) 387–395, <https://doi.org/10.1016/j.buildenv.2015.05.021>.
- [91] S. Administration, GB/T 17146, Test methods for water vapour transmission properties of building materials and products, 2015. (in Chinese).
- [92] P. Ren, C. Feng, H. Janssen, Hygric properties of porous building materials (V): comparison of different methods to determine moisture diffusivity, *Build. Environ.* 164 (2019) 106344, <https://doi.org/10.1016/j.buildenv.2019.106344>.
- [93] X. Guo, Y. Chen, Analysis of condensation in porous wall exposed to hot humid climate, *J. Civil, Arch. Environ. Eng.* 33 (2011) 121–142 (in Chinese).
- [94] G. Chen, Y. Chen, X. Liu, X. Guo, On the mould germination risk evaluation inside the hygroscopic wall in south of China, *J. Saf. Environ.* 17 (2017) 730–734 (in Chinese). <https://doi.org/10.13637/j.issn.1009-6094.2017.02.062>.
- [95] H. Viitanen, J. Vinha, K. Salminen, T. Ojanen, R. Peuhkuri, L. Paajanen, K. Lähdesmäki, Moisture and bio-deterioration risk of building materials and structures, *J. Build. Phys.* 33 (2008) 201–224, <https://doi.org/10.1177/1744259109343511>.
- [96] K. Sedlbauer, Prediction of mould fungus formation on the surface of and inside building components, Fraunhofer Institute for Building Physics, 2001.
- [97] F. Chen, Y. Liu, C. Ma, Y. Wang, D. Wang, Influence of moisture transfer on building enclosure's heat transfer coefficient among regional differences, *Build. Energy Environ.* 36 (2017) 6–11 (in Chinese).
- [98] F. Kong, Q. Zhang, Effect of new-completed building envelope heat and mass coupled transfer on thermalphysical parameters, *Acta Energ. Sol. Sin.* 34 (2013) 1930–1935 (in Chinese).
- [100] ISO 15927-3, Hygrothermal performance of buildings - Calculation and presentation of climatic data- Part 3: Calculation of a driving rain index for vertical surfaces from hourly wind and rain data, 2009.
- [101] H. Glaser, Grafisches verfahren zur untersuchung von diffusionsvorgänge, *Kältetechnik* 10 (1959) 386–390.
- [102] BS EN 15026, Hygrothermal performance of building components and building elements - Assessment of moisture transfer by numerical simulation, 2023.
- [103] J.R. Philip, D.A.D. Vries, Moisture movement in porous materials under temperature gradients, *Trans. Am. Geophys. Union* 38 (1957) 222–232.
- [104] J. Song, F. Liu, H. Bian, H. Wang, L. Zhang, The invention and application of simulation tool on coupled heat and moisture transfer in multiple wall, China, *Concr. Cem. Prod.* 63 (2015) 63–66 (in Chinese). <https://doi.org/10.19761/j.1000-4637.2015.04.016>.
- [105] X. Su, G. Li, W. Chen, Z. Jiang, Development of hygrothermal performance simulation software for building envelope, *New Build. Mater.* 38 (2011) 21–24 (in Chinese).
- [106] T. Kalamees, J. Vinha, Estonian climate analysis for selecting moisture reference years for hygrothermal calculations, *J. Thermal Env. Build. Sci.* 27 (2004) 199–220.
- [107] J. Koci, J. Madera, R. Cerny, Generation of a critical weather year for hygrothermal simulations using partial weather data sets, *Build. Environ.* 76 (2014) 54–61, <https://doi.org/10.1016/j.buildenv.2014.03.006>.
- [108] X. Zhou, D. Derome, J. Carmeliet, Robust moisture reference year methodology for hygrothermal simulations, *Build. Environ.* 110 (2016) 23–35, <https://doi.org/10.1016/j.buildenv.2016.09.021>.